

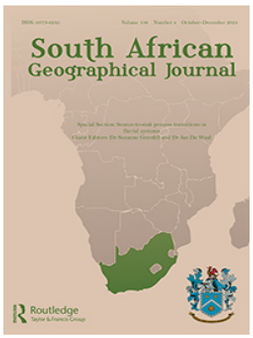
https://dspace.org/

Sediment source areas and the role of floods in sediments mixing on the Letaba River South Africa

Jasper Knight; Mary Evans; Tondani Mugwabana

https://hdl.handle.net/10539/41898
WOS

Downloaded from a DSpace repository. https://dspace.org/



South African Geographical Journal

ISSN: (Print) (Online) Journal homepage: www.tandfonline.com/journals/rsag20

Sediment source areas and the role of floods in sediment mixing on the Letaba River, South Africa

Jasper Knight, Mary Evans & Tondani Mugwabana

To cite this article: Jasper Knight, Mary Evans & Tondani Mugwabana (2024) Sediment source areas and the role of floods in sediment mixing on the Letaba River, South Africa, South African Geographical Journal, 106:4, 368-398, DOI: 10.1080/03736245.2024.2341656

To link to this article: https://doi.org/10.1080/03736245.2024.2341656

View supplementary material

Published online: 02 May 2024.

Submit your article to this journal

Article views: 55

View related articles

View Crossmark data

Citing articles: 1 View citing articles

Full Terms & Conditions of access and use can be found at
https://www.tandfonline.com/action/journalInformation?journalCode=rsag20

SOUTH AFRICAN GEOGRAPHICAL JOURNAL
2024, VOL. 106, NO. 4, 368–398
https://doi.org/10.1080/03736245.2024.2341656

Routledge
Taylor & Francis Group

Check for updates

Sediment source areas and the role of floods in sediment mixing on the Letaba River, South Africa

Jasper Knight, Mary Evans and Tondani Mugwabana

School of Geography, Archaeology and Environmental Studies, University of the Witwatersrand, Johannesburg, South Africa

ABSTRACT

The morphodynamics of rivers in semiarid environments tend to be controlled by episodic flood events, but the precise nature of sedimentary processes and sediment source areas within catchments affected by episodic floods remains not well understood. This study presents geomorphological, sedimentary and mineralogical data from different river reaches along the semiarid Letaba River within Kruger National Park, northeast South Africa. Geomorphological and sedimentary data were used to evaluate river morphodynamic behaviour and identify the major controls on landform development. Mineralogical data (heavy minerals and trace elements) were examined from surface sediment samples from different river reaches to determine the potential source areas for sediment reworking within the catchment (channel bank, channel bed, tributaries) for flood-transported sediments. Results of this analysis on downstream reaches show catchment-averaged sediment contributions from the channel bed of 42.5%, tributaries of 35%, and channel bank of 22.5%. These sediment contributions likely arise as a result of the different flow conditions experienced in different locations of the river system during floods. However, there is significant variability between samples from individual reaches, likely related to valley width and bedrock vs sediment availability. The contributions of river sediments from different sources are conceptually developed through a model of sediment source variability at different hydrodynamic stages. This highlights the role of floods in reactivating non-perennial tributaries and adding new sediment into the main channel. Measurements of perennial channel storage, therefore, do not give the whole picture of total sediment availability or activation during floods.

ARTICLE HISTORY
Received 23 June 2023
Accepted 26 March 2024

KEYWORDS
Fluvial geomorphology; river floods; sediment geochemistry; sediment source areas; semiarid rivers

1. Introduction

Semiarid areas commonly have highly seasonal rainfall patterns and these result in significant seasonal differences in river discharge and, thus, river morphodynamic behaviour (Grenfell & Ellery, 2009; Heritage et al., 2001c; Jury & Lucio, 2004; Rountree et al., 2001). The presence of low-density vegetation within the catchment often amplifies river response, leading to high sediment yield during flood events (Kotschy et al., 2000;

CONTACT Jasper Knight jasper.knight@wits.ac.za School of Geography, Archaeology and Environmental Studies, University of the Witwatersrand, Johannesburg 2050, South Africa
Supplemental data for this article can be accessed online at https://doi.org/10.1080/03736245.2024.2341656
© 2024 The Society of South African Geographers

Pollard et al., 2011). Several studies have examined the morphodynamics of flood events on the semiarid rivers of eastern South Africa (e.g. Heritage et al., 2001a, 2019, 2015; Knight & Evans, 2017, 2022; Milan et al., 2018, 2020; Smith & Zawada, 1990; Zawada, 1997). These studies show that flooding can not only result in sediment erosion and transport through the river system but that these geomorphic signatures vary spatially along different river reaches depending on valley width, the proximity of bedrock to the river channel, potential sediment availability, and river system morphometry including the number and size of feeder tributaries (Heritage et al., 2015). Flood signatures are, therefore, spatially variable, and their morphological and sedimentary signatures are influenced by past events, such as where a previous flood has removed much sediment from the system, leading to reduced sediment load in any subsequent flood event (Knight & Evans, 2018). These properties of semiarid rivers can be explained partly with respect to the differences between alluvial (mainly sand) and bedrock reaches, which respond in different ways to flood events by erosional stripping down to the underlying bedrock surface, and bedrock incision, respectively (Broadhurst & Heritage, 1998; Entwistle et al., 2014; Heritage et al., 2003; Rountree et al., 2000). The geomorphology of such 'mixed' river systems has been mapped across semiarid South Africa (e.g. Eze & Knight, 2018; Grenfell et al., 2014; Knight & Evans, 2024; Moon & Heritage, 2001; Rountree et al., 2000; van Niekerk et al., 1995). However, it is still uncertain how these patterns change over time as a result of flooding (Heritage et al., 2001c; Knight & Evans, 2024; Rountree et al., 2000, 2001) or by other mechanisms of catchment disturbance, including the spread of woody vegetation (Scholtz et al., 2014), drought conditions (Rountree et al., 2000), and longer-term climate variability (Heritage et al., 2001c). During flood events, sediment *in transit* through the river system can be derived from several potential source areas, including (1) the existing river channel bed, (2) areas outside of the existing river channel but located on the adjacent floodplain, (3) river terrace margins at the sides of the available floodplain, and (4) input from feeder tributaries (Baade et al., 2012; Collins et al., 1997; Hughes et al., 2022; Pulley et al., 2017). The relative contribution of sediments from these different source areas is not easily established because sediment's physical (e.g. grain size) and geochemical properties (e.g. heavy minerals, trace elements) are often quite uniform across a river catchment, especially where there is a single basement rock type or where chemical weathering has taken place over a long time (e.g. Chadwick et al., 2013; Silva et al., 2016). Sediment mixing models that are based on spatial variations in sediment properties have been used in many rivers worldwide (e.g. Collins et al., 1997, 1998, 2010; Cooper et al., 2015), including in South Africa (e.g. Manjoro et al., 2017; Pulley et al., 2017). In these studies, different modelling approaches have been used, including Monte Carlo, discriminant function analysis, and Bayesian analysis (e.g. Davies et al., 2018; Patault et al., 2019; Pulley et al., 2020; Vale et al., 2020) as well as different numerical mixing models (see discussion in Dai et al., 2022). As input variables, these studies have used different mineral and trace elements, radionuclides, and stable isotopes (e.g. Vale et al., 2022). However, these approaches need systematic and consistent sediment sampling through a river system, which is often difficult to achieve, and works less well in semiarid areas such as in South Africa where seasonal flood events characterize the river regime. For this reason, a mixing model approach is not applied in the strictest sense in this study. Instead, sediment tracing of the main channel and tributaries is used to support evidence from river reach geomorphology, sedimentology

and geochemistry. This means that the specific methodologies developed in previous mixing studies cannot be always easily applied to all contexts.

The major aim of this study is to evaluate the morphodynamic behaviour and major controls on landform development within the semiarid and perennial Letaba River (northeast South Africa). This is achieved through grain size and geochemical analysis of sediment samples collected through the river system (Mugwabana, 2018), including evaluating the contribution of sediments from its ephemeral tributaries. The data on mineral composition and trace element concentrations within individual samples are then used to identify spatial variations in sediment source areas. This is achieved through a modified mixing model procedure. The degree and style of sediment reworking down the river system are then evaluated based on reach geomorphology and sediment properties.

2. Study area

The east-flowing Letaba River is situated in the northeastern part of South Africa (Figure 1) and has a total catchment area of 13 670 km^2 (State of the Rivers Report, 2001). Of this, 3300 km^2 is located within the protected nature reserve of Kruger National Park (KNP) (Kotschy et al., 2000). Headwater areas of the Eastern Escarpment mountains are underlain by granite, quartzites and sedimentary rocks of the Karoo Supergroup (Schutte, 1986; Viljoen, 2015). This part of the catchment (the Groot Letaba) is dominated by commercial forestry, and river geomorphology comprises pool-and-riffle bedrock reaches with disconnected sediment bars and floodplain elements at footslope locations (Moon & Heritage, 2001). Middle reaches of the Letaba on the South African Lowveld (mainly 600–1300 m asl) are developed in granite and gneiss bedrock with dolerite dikes and basalt beds (State of the Rivers Report, 2001) and have mixed braided to anastomosing river channels. Commercial forestry, subsistence agriculture and irrigated commercial farming are practised within this part of the catchment. Dams are common along this river stretch. The Klein Letaba and Groot Letaba tributaries join at the western border of KNP (Figure 2) to form the Letaba River proper. Within KNP (mainly at 200–400 m asl), the underlying bedrock is mainly basalt (Bristow et al., 1986). Bedrock outcrops of different geologies are found throughout the Letaba River system, thus it can be classified as alluvial to mixed bedrock/sediment type (Moon & Heritage, 2001) where bedrock surfaces are covered with loose alluvial sediments that can be rapidly moved by floodwaters. In detail, the area upstream of sampling site 7 (Table 1) is mainly dominated by Archaean-age Makhutswi gneiss whereas the area downstream of this site is mainly underlain by olivine-rich basalts of the Letaba Formation. The varied rock types throughout the catchment have different properties with respect to their mineralogy and trace element geochemistry (Bristow et al., 1986; Erlank, 1984). Close relationships also exist between bedrock geology and overlying soils (Venter, 1986) and ecosystems (Munyati et al., 2013). This variability means that one would anticipate that different tributaries, sourcing different bedrock types, should have different geochemical compositions.

Average annual precipitation and potential evapotranspiration across the catchment is 612 mm and 1669 mm, respectively, meaning that there is a significant overall water

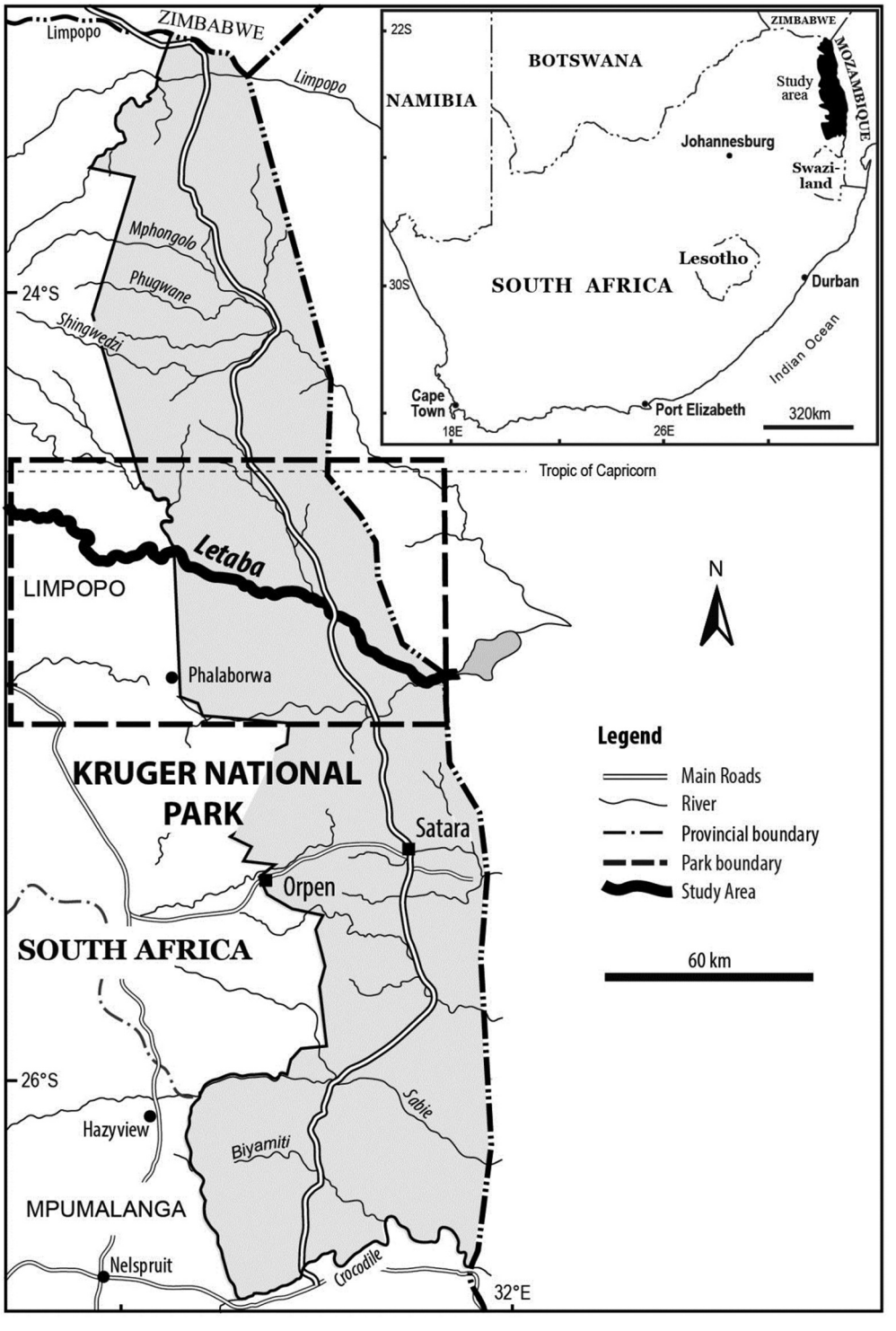


Figure 1. Location of the lower Letaba River (boxed) within the Kruger National Park and South Africa.

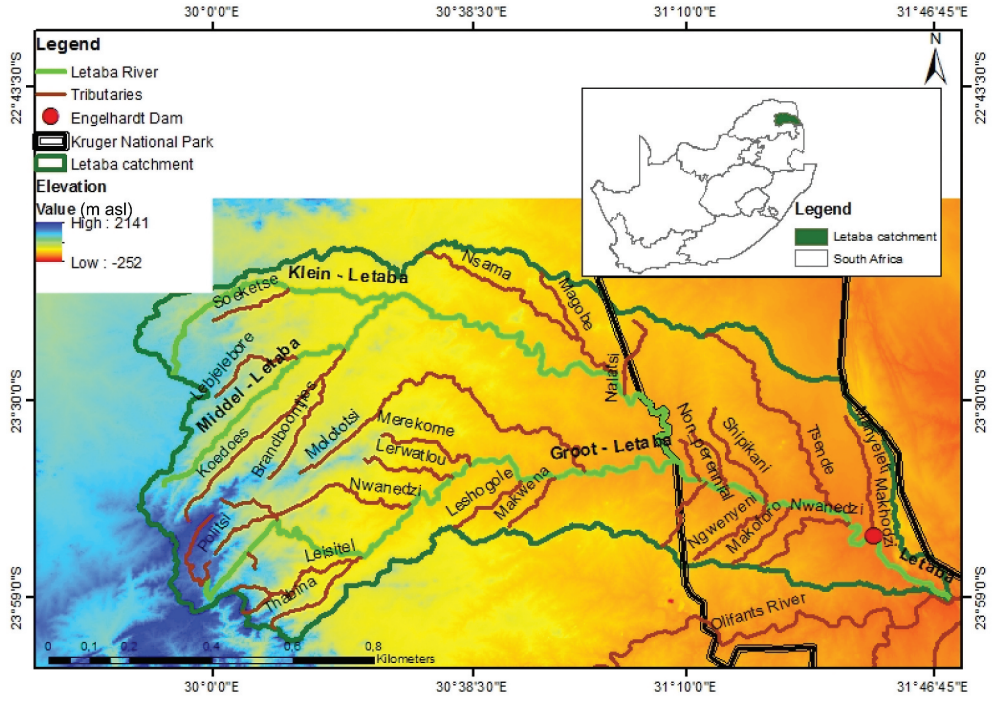


Figure 2. Topographic context of the Letaba River catchment and its major tributaries. The eastern half of the catchment flows through the Kruger National Park.

deficit (State of the Rivers Report, 2001). However, annual precipitation across the catchment is highly variable, with headwater areas receiving >1800 mm of precipitation per year but lowland areas within KNP falling within a semiarid zone and receiving <450 mm of precipitation per year. This results in a significant west – east precipitation gradient (Moon & Heritage, 2001). This also means that 6% of the total catchment area produces more than 60% of the river's mean annual runoff (State of the Rivers Report, 2001). This spatial variability suggests that different sub-catchments within the Letaba watershed may experience significantly different rainfall amounts and waterflow conditions, with implications for sediment transport processes and patterns within different tributaries. Precipitation in the region occurs mainly during the austral summer months (October to March) (Jury & Lucio, 2004), and such seasonal floods have a major impact on river morphodynamics in the region (Heritage & Moon, 2000; Rountree et al., 2000; Heritage et al., 2001b, c, Pettit et al., 2005; Cunningham et al., 2015; Saraiva Okello et al., 2015; Knight & Evans, 2017). This is confirmed by hydrograph data from the Letaba River that show peak flows in January/February of the years 2006, 2011, 2013 and 2014 (which includes the sampling period of this study, of Sept/Oct 2015) (Figure 3). More recent events include high rainfall and river floods associated with cyclones Dineo (February 2017), Idai (March 2019) and Freddy (February 2023). The highest peak discharge volumes in the 2006–15 record were experienced at the Engelhardt Dam gauge station (station B8H018) in 2013, with monthly total discharge reaching 563 m^3. Downstream reaches also experienced higher discharge volumes. The mixed bed of the

Table 1. Description of study sites along the Letaba River, South Africa. The rows shaded grey indicate samples collected from tributaries.

Site #	Location	Geomorphic and locational setting	River geomorphic type	Features observed
1	23°38.920′S, 31°08.750′E	Confluence of Klein Letaba and Groot Letaba	Alluvial single thread	3D subaqueous dunes overlain by mud drapes with desiccation cracks, granitic gneiss outcrops, vegetated sandbars, steep terrace valley sides
2	23°41.462′S, 31°11.905′E	At unnamed non-perennial tributary	Alluvial single thread	Steep and narrow erosional valley sides, coarse sandy bedforms, no floodplain present
3	23°42.730′S, 31°17.282′E	At Shambali River tributary	Alluvial braided	Steep and erosional valley sides, coarse sandy bedforms, granitic gneiss boulders
4	23°42.730′S, 31°17.284′E	Along the main Letaba River at Shimuwini Dam	Alluvial braided	Channel is sediment-dominated, isolated bedrock outcrops are present on valley margins. Vegetated sandbars separate multiple channels. A wide floodplain exists covered by thin flood sand sheets
5	23°45.531′S, 31°22.281′E	At Mopani/Phalaborwa bridge	Bedrock anastomosing	Narrow river channel, inactive sandbars, clast lags and gravel bars
6	23°45.680′S, 31°25.610′E	At non-perennial Makoforo River tributary	Alluvial braided	Multiple channels separated by large sandbars, inactive vegetated bars present, narrow valley with steep sides
7	23°46.166′S, 31°30.637′E	Along the main Letaba River	Alluvial braided	Multiple sandbars and channels, large sandstone outcrops are present at the valley margin and contain very large (3 m wide, 5 m high) potholes. Wide floodplain with thin flood sand sheets
8	23°48.640′S, 31°33.929′E	In Nwanedzi River tributary	Alluvial single thread	Steep and narrow erosional valley sides, coarse sand plain and gravel lag in the dry river channel, no floodplain present
9	23°50.149′S, 31°34.990′E	Along the main Letaba River	Alluvial single thread	Sinuous main channel and flat-topped sandbars, wide floodplain with steep valley margins
10	23°50.199′S, 31°37.736′E	Along the main Letaba River	Alluvial single thread	Very wide, flat and vegetated floodplain
11	23°50.279′S, 31°39.182′E	Along the main Letaba River, downstream of the Engelhardt Dam	Mixed bedrock-alluvial anabranching	Eroded sandbars and bedrock outcrops, river channels are bedrock controlled, valley is wide but with anabranching bedrock channels and steep valley margins
12	23°53.241′S, 31°39.182′E	Along the main Letaba River	Mixed pool-rapid	Basalt bedrock within the main channel, wide and generally flat floodplain with thin sand sheets and gently sloping valley margin
13	23°54.873′S, 31°41.633′E	Along the main Letaba River	Bedrock anastomosing	Diorite outcrops with coarse sandbars in between them, anabranching channels controlled by bedrock, wide valley with sloping but vegetated margins
14	23°54.594′S, 31°43.869′E	Along the main Letaba River, at low-water bridge	Mixed bedrock-alluvial anabranching	Broad coarse sandbars with basalt bedrock outcrops at valley margins and occasionally on the floodplain, thick sand sheets, wide valley with gently sloping margins
15	23°56.819′S, 31°44.318′E	Along the main Letaba River	Mixed bedrock-alluvial anabranching	Isolated basalt bedrock outcrops, very wide and flat floodplain, extensive boulder lags near valley margins, broad and low coarse sand bars

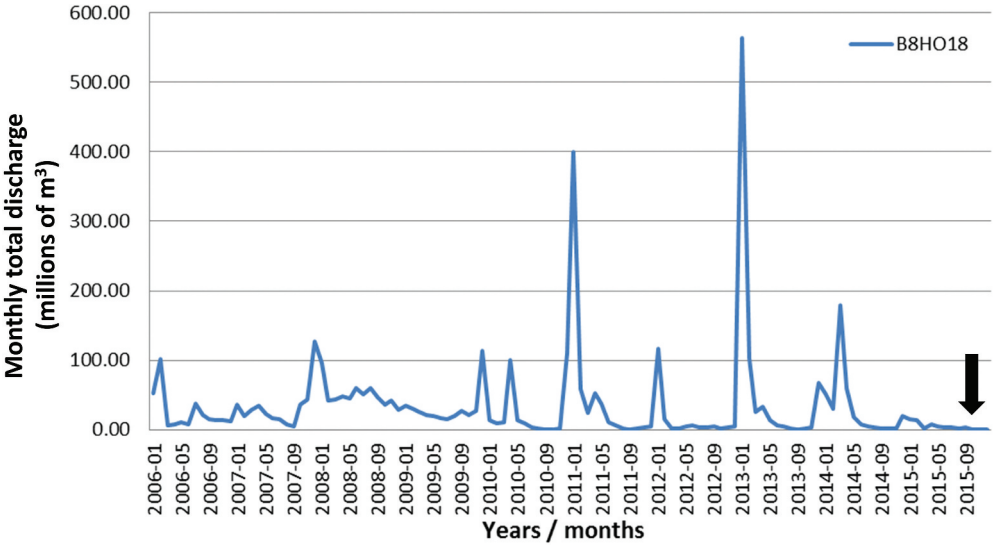


Figure 3. Graph of historical river discharge recorded at the Engelhardt Dam gauging station (B8H018) on the lower Letaba River (location is marked in Figure 2), for the period 2006–15, including the sediment sampling period in this study (indicated with the black arrow). Values represent total monthly water volumes in millions of m^3.

Letaba River means that bedrock and sandy reaches respond to flood events in different ways (e.g. Milan et al., 2020; Moon & Heritage, 2001).

3. Methods

3.1. River geomorphology mapping

The Letaba River within KNP (~95 km distance) was mapped for river geomorphology based on (1) analysis of Landsat 8 imagery (pixel resolution: 30 m, date of acquisition: 30 September 2015); and (2) field mapping and validation in the field (30 Sept–2 Oct 2015), during the driest part of the year and after the last geomorphologically-significant floods in the catchment in January 2014 (see Figure 3). Landsat images were pre-processed using ENVI v5.2 with steps including atmospheric correction (using Gram-Schmidt pan-sharpening), mosaicking and colour balancing using ENVI, and then on-screen digitizing of different channel types using ArcGIS v10.3.

Five main channel types were identified and mapped through the Letaba River, based on classifications used in a previous study on Letaba River geomorphology by Moon and Heritage (2001) (see also Knight & Evans, 2024). These channel types are bedrock anastomosing, alluvial braided, mixed pool-rapid, alluvial single thread, and mixed bedrock-alluvial anabranching. These channel types are distinguished by the presence/absence of different geomorphological features such as braid bars, rock pools, boulder beds, terraces, or river channel patterns. These channel types have also been identified by mapping different reaches of the Sabie and Limpopo rivers in this semiarid region (Eze & Knight, 2018; Knight, 2022).

Field validation of remote sensing mapping was achieved at 15 sites representing different river reaches along the Letaba River within KNP (sites 1–15 marked in

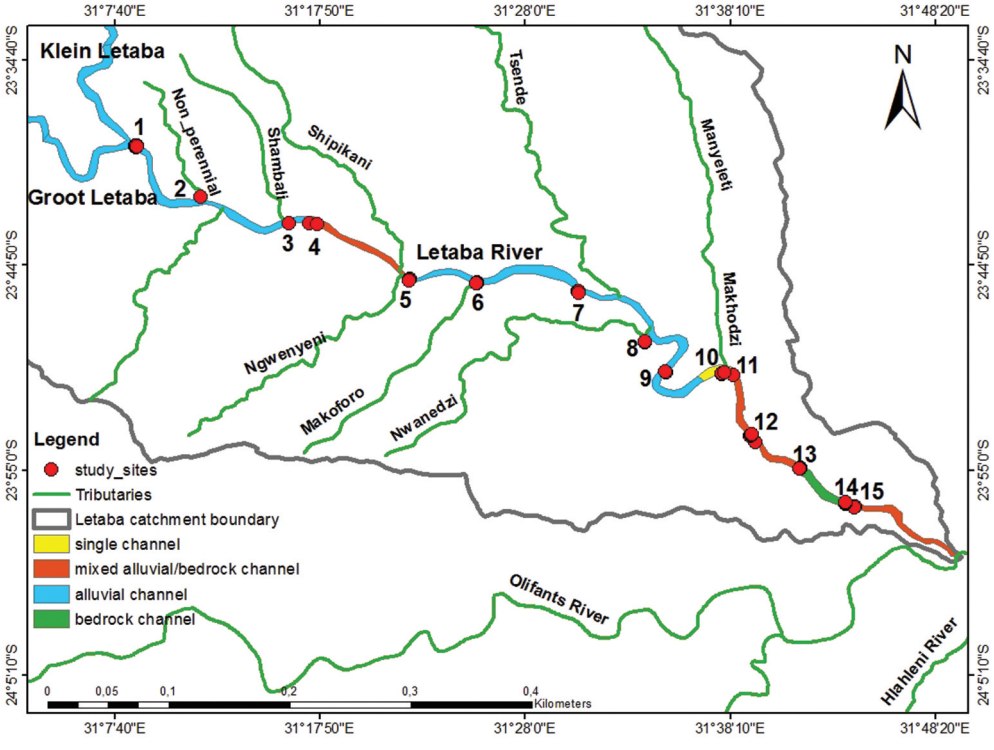


Figure 4. Map of the lower Letaba River within Kruger National Park, showing the geomorphic classification of river reaches (based on Moon & Heritage, 2001, and updated with mapping in this study), and the locations of sites 1–15 (see Table 1).

Figure 4). The sites were chosen to reflect the range of different channel types present. Site locations were logged using a differential GPS (positional accuracy ±3 cm). Geomorphological features such as in-channel and flood bars, terraces, floodplains, levees, reworked aeolian sand dunes and crevasse splay deposits, characteristic of each channel type, were mapped along the area of interest.

3.2. Field sampling

Bulk surface sediment samples (~500 g) in the sand size fraction (which is almost exclusively the size fraction present here) were collected at each field site to analyse grain size differences and changes in heavy mineral proportions across and along the river. In total, 49 sediment samples were collected across the 15 sites from locations immediately adjacent to the active channel. The number of samples taken at each site ranged from two to four. Sediment samples were also collected from previously active (but now dry) channels within adjacent ephemeral tributaries. This sampling strategy was consistently applied through the entire river system. The geomorphic context of each sample was noted, including the presence of bedrock outcrops or sediment landforms within and around the active channel and across the floodplain. Sample locations were logged using a differential GPS. Bedrock geology was noted where exposed.

3.3. Sediment properties

Bulk sediment samples collected in the field from the active or previously active channels were examined in the laboratory for grain size distributions using the sieve technique at 0.25 phi intervals from 2 mm to 63 μm. Results were analysed using the Gradistat software (Blott & Pye, 2001) which calculates statistical parameters such as the mean, mode, sorting, skewness and kurtosis for each sample using the Folk and Ward (1957) method. Sediment samples were also evaluated for their combustible organic content using the loss on ignition method, in which a subsample was burnt in a muffle furnace at 420°C for 8 h.

3.4. Sediment mineralogy

Following sieving, grains in the size range 63 μm to 2 mm from each sample ($n = 47$, two samples did not yield enough fines) were placed on a glass slide (46 × 26 mm) containing oil for mounting, covered by a cover slip, and heated before analysis. Between 300 and 500 grains were present on each glass slide. One thin section was prepared for each sample by polishing, and the slide was examined using a petrographic microscope. Minerals were identified and counted based on mineral properties including colour, pleochroism, habit, cleavage, twinning, relief, Becke line and birefringence (Lynn et al., 2008). Images of the samples were taken using an Olympus DP2 Twain camera together with the AnalySIS getIT v5.2 software. Minerals such as magnetite, ilmenite and haematite were identified under reflected light at a magnification of 40×, and other minerals (olivine, clinopyroxene, orthopyroxene, biotite, muscovite, hornblende, rutile, zircon, tourmaline, zoisite, plagioclase and orthoclase) were identified under transmitted light at a magnification of 4× and 10×. Between 200 and 300 mineral grains were counted on each slide.

3.5. Elemental analysis

For each sample where enough fine sediment was present ($n = 46$), the <63 μm size fraction was analysed using X-ray fluorescence (XRF) spectroscopy, which is a standard methodological approach (e.g. Smith et al., 2018; Vale et al., 2022). A standard pellet of 5 g was used. Major elements within each sample were obtained by the fusion method with a tetra-borate flux using the SuperQ® program, while trace elements were analysed by the pressed pellet method with an organic binder (MOWIOL), using the ProTrace® program. Data are reported as % (for major elemental concentrations) and ppm (for trace element concentrations) (see supplementary data files A and B).

3.6. Sediment source samples

Three potential sediment source areas for river sediments are considered in this study: tributaries, the channel bank (including any eroded floodplain margin), and the channel bed. This was a deduction based on field observations of river geomorphology. In addition to the samples collected from the active/inactive channels, control samples ($n = 8$) from the three proposed source areas were also collected.

Tributary samples were collected from sites 1, 2, 6 and 8 (locations shown in Figure 4), channel bank samples from sites 1 and 9, and channel bed samples from sites 4 and 8. Pulley et al. (2017) and Smith et al. (2018) discussed the importance of choosing the most appropriate source areas and proxy indicators for any given study; here, we are confident that we have done so because our choice of source areas was based on an understanding of the local river geomorphology as well as on the seasonal variations in river discharge experienced by the main river channel and by its ephemeral tributaries (cf., Heritage et al., 2001b; Moon & Heritage, 2001). As with surface samples from the contemporary river system, sediment from potential source areas was analysed using XRF for bulk and trace element concentrations. The mean and standard deviation of trace element concentrations were analysed in order to evaluate elemental variability between samples, with high variability implying that the sediment can be distinguished according to its different sources (e.g. D'Haen et al., 2012; Walling et al., 2008). Only those trace elements that display statistical significance with respect to different source areas were chosen for further analysis (see supplementary data file B) because these represent the diagnostic indicators to use to geochemically fingerprint river samples back to their source areas (e.g. Collins & Walling, 2002; D'Haen et al., 2012). This methodology is the same as has been used in other studies on fluvial sediment sources (e.g. Manjoro et al., 2017; Nosrati et al., 2018; Patault et al., 2019) and more recently in a study on sediment source contributions into KNP dams (Miller et al., 2022).

3.7. Distinguishing sediment source areas

Sediment provenance studies involve identifying potential sediment sources, selecting properties which can discriminate between these sources, and comparing these properties to those of the river sediment samples (Walling et al., 2008). A sediment mixing model approach can identify the relative contribution from potential sediment sources. The mixing model used in this study is the modified Collins model (Haddadchi et al., 2013), chosen because it has been successfully used to identify river sediment sources in previous studies (e.g. Collins et al., 2010; Haddadchi et al., 2013, 2014). Two statistical tests of the tracers were conducted in order to determine which to use in the mixing model. These were the Kruskal Wallis H-test and stepwise multivariate discriminant function analysis. The Kruskal Wallis test identifies tracers that can discriminate between different sediment sources. Discriminant function analysis then tests the trace elements that pass the Kruskal Wallis test, and the number of tracers which are correctly classified into the potential source category (Manjoro et al., 2017). The results of the discriminant function analysis are based on the Wilk's lambda algorithm which indicates the tracers which are correctly classified into the potential source groups.

Collins et al. (2010) proposed a modified mixing model (Eq. 1) which was used in this study to identify potential sediment sources along the Letaba River. Within this model, the source type contributions must all be positive and the total of the source type contributions must be equal to 1 (Collins et al., 1997).

$$\sum_{i=1}^{n}\left\{\left(C_i-\left(\sum_{s=1}^{m}P_sS_{si}Z_sO_sSV_{si}\right)\right)C_i\right\}^2W_i \quad (1)$$

where C_i = concentration of fingerprint property (e.g. concentration of trace elements); (i) is the floodplain sediment collected from the sub-catchment outlet; P_s = the optimized percentage contribution from source category (s); S_{si}=mean concentration of fingerprint property (i) in source category(s); Z = particle size correction factor for source category (s); O = organic matter content correction factor for source category (s); SV_{si} = weighting representing the within-source variability of fingerprint property (i) in source category (s); W_i=tracer discriminatory weighting; n = number of fingerprint properties comprising the optimum composite fingerprint; m = number of sediment source categories.

The model was run in Python v2.7.8 with iterations repeated for each trace element at each source category so as to calculate the source contributions. In order to understand sediment sources in a downstream direction, the model needs to be applied using source samples that lie upstream of each site, thus the model was only run for sites that are located downstream of the sampled source sites. These upstream sediment source samples provided a suitable number of samples in order to calculate the parameters that were needed to run the model. The relative source apportionments from each source were estimated by calculating the overall mean estimated contribution from each source and dividing it by the estimated mean obtained from each source for all the sediment samples collected from the different sites. The accuracy of the model was assessed using the Mean Absolute Error (MAE) (Haddadchi et al., 2014; Hughes et al., 2009) for individual and group sediments according to (eq. 2):

$$\mathrm{MAE}=\frac{\sum_{j=1}^{m}\left|X_{j-}Y_j\right|}{m} \quad (2)$$

where X_j is actual percentage of sources in mixture sediments, Y_j is calculated contribution of each source (j) and m is the number of sources ($m = 3$). Walling and Collins (2000) indicated that, in order for the model results to be considered as reliable, the errors must be < 15%.

4. Results

4.1. River geomorphology

Reach-scale geomorphology of the Letaba River is presented in Figure 4, based on Landsat data and field mapping. Alluvial and mixed bed types are most common in terms of the river length occupied by these types. Meandering channels and vegetated sandbars characterize alluvial channels. Diorite and basalt outcrops are found in bedrock-influenced reaches. A summary of the geomorphic context and properties of surface sediments and landforms found at the 15 sampled sites is shown in Table 1 where examples of all five geomorphic categories recognized by Moon and Heritage (2001) are identified. Individual river reaches vary in geomorphic properties; representative photos of channel types from the Letaba system are presented in Figure 5.

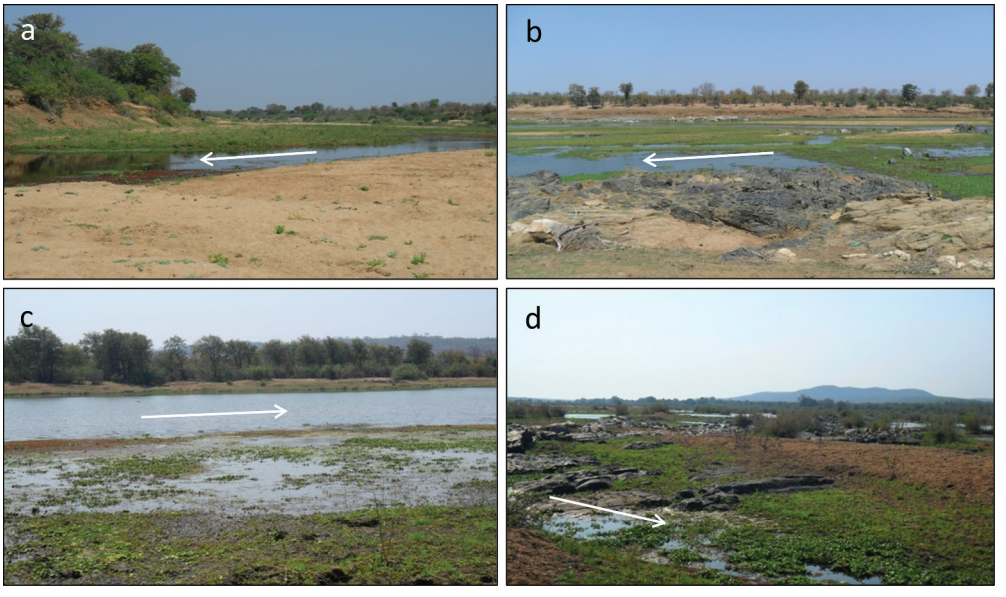


Figure 5. Field photos from the Letaba River. (a) The Groot Letaba River (site 1) with a vegetated sandbar alongside the active channel; (b) vegetated sandbars separating multiple channels (site 4); (c) a single, straight deep channel with a wide, flat, vegetated floodplain (site 10); (d) bedrock outcrops and isolated sediment patches (site 15). Arrows show water flow direction.

4.2. Grain size properties and patterns

Grain size properties show high spatial variability through the Letaba River system. Overall, sediments are moderately sorted to moderately well sorted, representing 45% and 33% of all samples, respectively. This variability is also reflected in values of kurtosis, skewness and sorting (Figure 6). Median grain size generally increases in a downstream direction from site 1 at the Klein Letaba/Groot Letaba confluence (Figure 7), which is largely the result of the input of coarser sediment from incoming tributaries and which is also reflected in other sediment properties (Table 2).

4.3. Mineral analysis

The abundance of different minerals observed by petrographic microscope, from different sites in the Letaba River system, is shown in Table 3. The most abundant mineral is quartz, followed by biotite and muscovite. Opaque minerals make up between 11.6% to less than 1%, with magnetite being the most dominant. Grain sizes of individual minerals vary at different river reaches; examples of different sizes of olivine grains can be seen in Figure 8(i, n). Minerals such as zircon also exist as inclusions in quartz grains (Figure 8(a–d)). Site 1 at the confluence of the Groot Letaba and Klein Letaba is underlain by migmatised biotite gneiss and, thus, there is an abundance of locally derived orthopyroxene and muscovite at this site, with orthopyroxene making up 33.2% of the mineral grains counted. Site 4 is underlain by granodiorite and contains high values of magnetite (7.4%), biotite (17.8%) and muscovite (12%). Site 7 is underlain by fine-grained sandstone and siltstone and the sample

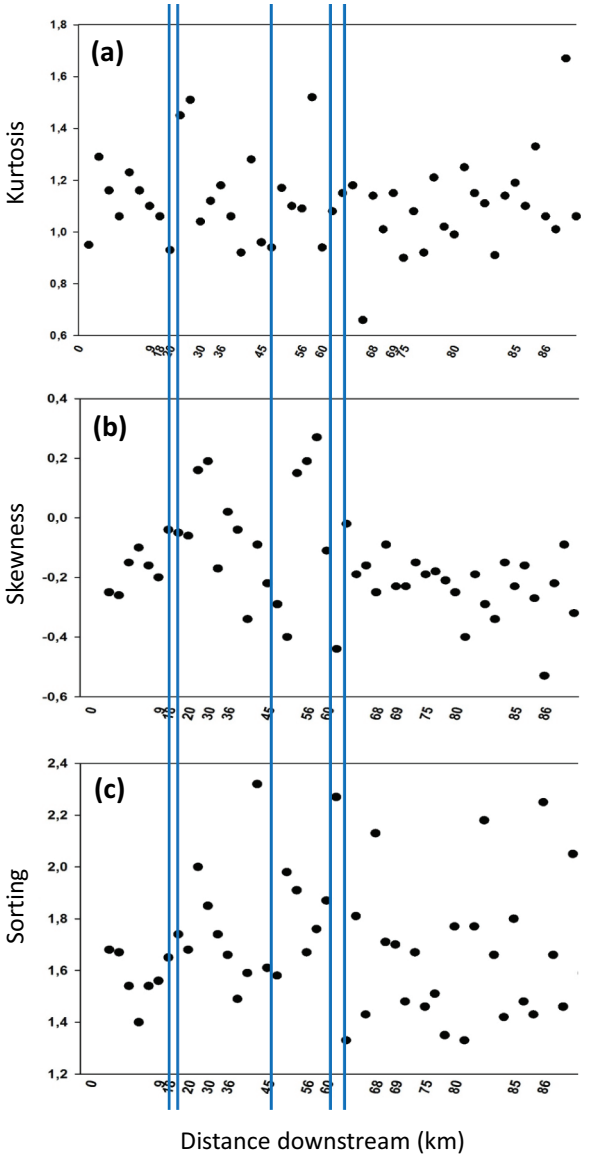


Figure 6. Scatterplots of (a) kurtosis, (b) skewness and (c) sorting of sediment samples from the Letaba River, arranged in a downstream direction from site 1. The vertical blue lines indicate the major tributaries as locations of sediment input (named in Table 1).

from this site is abundant in clinopyroxene (4.9%) and micas (31.2%) derived from these rocks. The sediment at site 9, which is underlain by basalt, is abundant in olivine (2.7%), biotite (6.3%) and magnetite (3.4%). Sites 1 and 14 appear to be enriched from a similar source because of the presence of abundant orthopyroxene. The highest proportions of magnetite, ilmenite and haematite are found at sites 4, 5 and 13.

The tributaries pass through areas of similar bedrock geologies to the main Letaba River catchment. Site 2 is a non-perennial tributary (Table 1). The

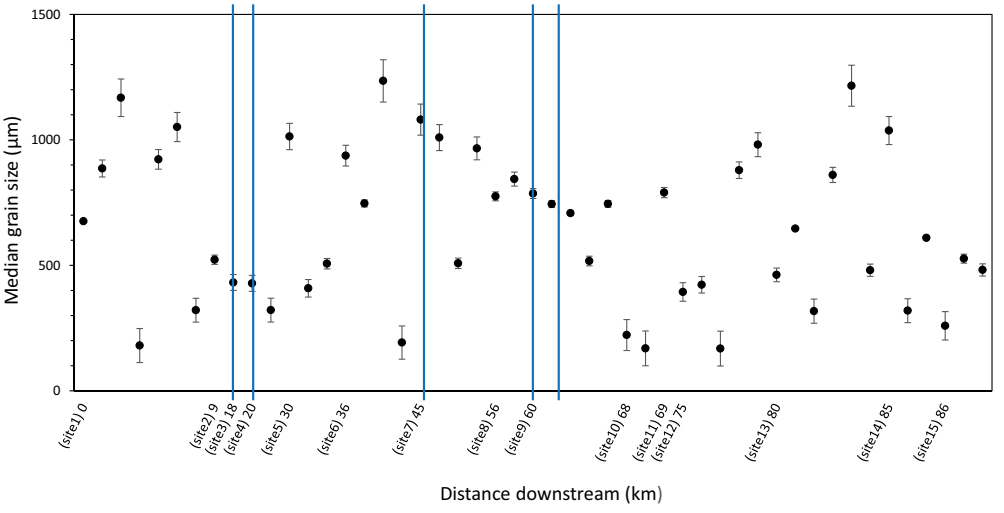


Figure 7. Scatterplot of median grain size (µm) of sediment samples from the Letaba River, arranged in a downstream direction from site 1. Error bars indicated one standard deviation. The vertical blue lines indicate the major tributaries as locations of sediment input (named in Table 1).

Table 2. Comparison of sediment properties from surface sediment samples taken immediately before (upstream) and after (downstream) the major tributaries along the Letaba River.

	Site 1		Site 6		Sites 10 and 11		Sites 12 and 13	
Grain size properties	Before	After	Before	After	Before	After	Before	After
Median grain size (µm)	709	292	1121	834	434	980	387	767
Sorting	1.647	1.576	1.594	1.396	1.590	1.667	1.484	1.719
Skewness	−0.041	−0.298	−0.342	−0.103	−0.229	−0.154	−0.058	0.157
Kurtosis	1.097	0.959	1.056	1.057	1.080	0.899	0.929	1.446
n	1	1	3	6	2	1	5	6

sediment in this dry river bed is abundant in olivine (7.5%), clinopyroxene (6.4%) and muscovite (8.4%) (Table 3). Site 3 is the non-perennial Shambali River tributary which is underlain by coarse-grained gabbro. The sediment in this tributary is abundant in large subhedral clinopyroxene grains (7%), and columnar zircon grains (3.5%) that are present as inclusions within quartz grains. Subhedral zoisite grains around 2 µm in size make up less than 1% of the minerals present (Figure 8(f)). Site 8 is the Nwanedzi River which is one of the largest tributaries entering the Letaba River and is underlain by basalt. The river sediment here is abundant in olivine (5.2%), biotite (9.9%), muscovite (7.2%) and rutile (6.7%) (Table 3). The large olivine grains have a fine-grained groundmass of euhedral plagioclase (Figure 8(n)). The Makoforo River enters the Letaba River at site 6 and is underlain by tonalitic biotite gneiss. Sediment from this tributary is abundant in rutile (4.1%) and biotite (4.8%). Zircon is present as parallel-aligned inclusions within quartz grains. The non-perennial Shambali and Makoforo rivers contain very low percentages of magnetite, ilmenite and

Table 3. Table indicating the number of individual mineral grains recorded in samples from different river reaches (qtz = quartz, plag = plagioclase, ortho = orthoclase, cpx = clinopyroxene, olv = olivine, hbld = hornblend, bt = biotite, mg = magnetite, il = ilmenite, hm=hematite, opx = orthopyroxene, msc = muscovite, epd = epidote, zirc = zircon, rt = rutile, tour = tourmaline, zoi = zoisite, gt = garnet). The rows shaded grey indicate samples collected from tributaries. Blank cells indicate that these minerals were not observed in the sample slide. n = total number of grains counted on that slide.

Site	qtz	plag	orth	cpx	olv	hbld	bt	mg	il	hm	opx	msc	epd	zirc	rt	tour	zoi	gt	n
1	150	10		13	4	7	22	23	8	10	138	13	5	4	9				416
2	201			24	28	7	7	12	3	3	10	30	3	10	30	3	1	1	373
3	171	15	6	20	2		20	8	2	4	10	15		10					283
4	311	5		17		3	111	46	14	33		75	7	13	8				623
5	263					13	68	70	25	35		40	20	11	51	6			602
6–4	282			9	5	5	18	8	4	3	2	8	7	4	15				370
6	388		4	23	5	7	70	9	3	4	11	32	8	4	39	2	2		611
7	273	2		31	2	9	102	27	13	15	9	95	22	1	20	7	4	1	632
8	174	9			21	12	40	18	16	16	15	29	9	13	27	2			401
9	342	10		11	15	8	35	19	7	10	6	36	25	8	16	6	4	1	559
10	221		5	12	5	3	18	17	8	11	11	29	10	6	9		2		367
11	239	6		28	15	9	122	9	5	10	10	96	43		73	19	1	4	689
12	235			24	5	10	58	20	10	10	7	36	14	12	34	10			485
13	266	15	5	28	14	5	12	42	11	19	19	28	7	6	13		2	3	495
14	212		3	5	9	8	18	9	4	5	38	15	10	15	14		2		367
15	219	6		35		13	177	21	7	9		33		4					517

haematite (0.8 to 3.2%). The Nwanedzi River (site 8) contains high values of magnetite (4.4%), ilmenite (3.9%) and haematite (3.9%) when compared to other tributaries.

Following analysis of the <63 μm fraction, the concentration of trace elements present in the sediment samples is indicated in Figure 9 (see supplementary data file A). The most abundant trace elements are Zr, Ba, Cr and Sr, but these are present in different quantities at different sites. It is notable that some trace elements show very little variability through the river system, in particular Sr, Ba, and those at very low concentrations. The greatest variability exists in Zr and Cr, and some isolated peaks in Ni and Ga. Peaks in the abundance of Zr correspond in particular to sediment contributions from tributaries at sites 2 and 6. At site 6, high concentrations of V, Cr, Co, Ni, Sr, Y, Zr, Nb, Mo, Ba, Th and U reflect sediment input from the Makoforo River tributary, and the concentrations of these trace elements decrease with distance as their sediments mix with Letaba river sediments. High concentrations of Cr (466 and 623 ppm) and Ni (237 and 198 ppm) were sampled from the Nwanedzi River (site 8), which enriches the Letaba River with these elements. Correlation coefficients between different trace elements show that a positive relationship exists between Sc, V, Co, Cu, Zn, Y, Ga and Nb (supplementary data file A). A strong correlation coefficient of 0.91 exists between Sc and V. A positive relationship also exists between Th, Cr, Zr, Y, Ni, Pb, U and Ga (0.52 to 0.71). Correlation coefficient analysis was then used to examine the relationships between trace elements and heavy minerals composition (supplementary data file B). There are statistically-significant ($p > 0.5$) positive relationships between garnet and Sr, zircon and Mo, Sr and Zr, and magnetite and Nb. There are statistically significant ($p > 0.5$) negative

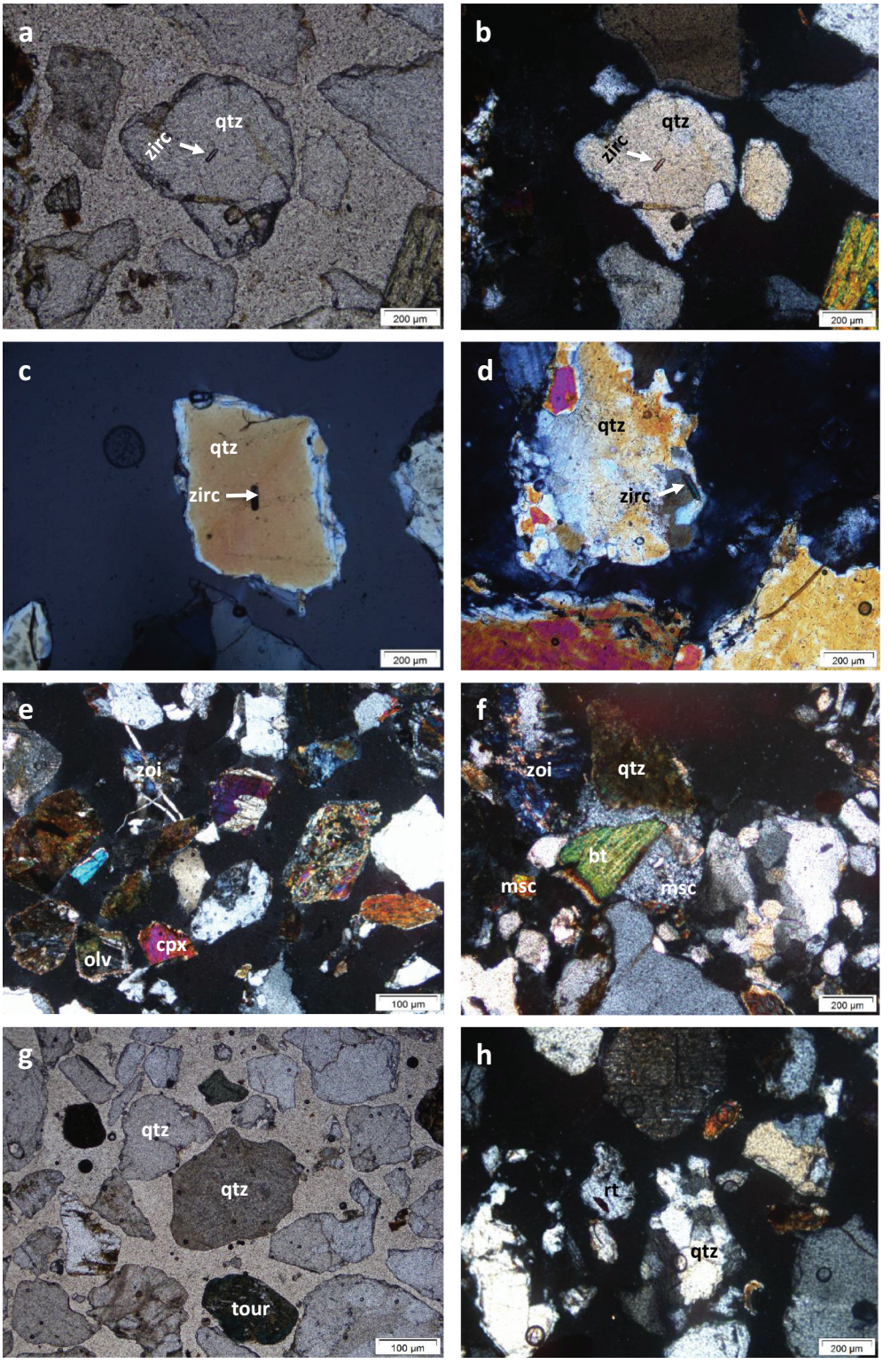


Figure 8. Images from polished slides indicating minerals present in the sediment. (a, b) Columnar zircon inclusion in a quartz grain from site 10, in plain light (a) and crossed polar (b), (c) zircon

relationships between zoisite and V, Cu, Zn and Ga, garnet and Ga, and plagioclase and Mo.

It is important to note elements with the highest overall concentrations are not always the most useful indicators for discriminating between sources, but rather those with the greatest variability (Pulley et al., 2017). Results from sites 10 and 12–15 are presented because these sites lie immediately downstream of the source samples analysed. Contributions from tributaries are highest at sites 10 and 15, channel banks are highest at site 13, and channel beds are highest at sites 12 and 14 (Table 4 and Figure 10). Values for the Letaba River as a whole, when all analysed samples are averaged, show a clear mix of sediment sources (Table 4). Mean Absolute Errors were calculated for each of the potential source areas (Figure 11). The model indicates high accuracy values with the median error values for channel bank, channel bed and tributary of 43%, 33% and 36%, respectively. A few of the samples had accuracies of less than 10%, but most samples had high accuracy values (40–50%), indicating that the model estimated the percentage source contributions reasonable well. Note that these accuracy values lie commonly above Walling and Collins' (2000) recommended threshold of 15%.

5. Discussion

Several studies have examined the geomorphology and dynamics of South Africa's semiarid rivers (e.g. Entwistle et al., 2014; Grenfell & Ellery, 2009; Heritage et al., 2001a, 2015; Heritage & Moon, 2000; Heritage & van Niekerk, 1995; Moon & Heritage, 2001; Tooth et al., 2004). Heavy rainfall events and associated flooding are major controls on river dynamics in semiarid regions, including in KNP (Heritage et al., 2021b, 2021c, 2015; Knight & Evans, 2017, 2018, 2022, 2024; Milan et al., 2018; 2020; Spaliviero et al., 2014). This control is discussed in several previous papers (e.g. Heritage et al., 2001b, 2001c, 2003, 2004, 2015; Jury, 2016; Jury & Lucio, 2004; Odiyo et al., 2015) and is confirmed in this study by the significant role of sediment contribution to the Letaba River system by ephemeral tributaries (Table 4) that are activated (i.e. contribute sediment into the main perennial channel) by flood events.

5.1. The role of river floods in sediment source switching

Low-flow regimes on KNP rivers (1–2 m s^{-1}; Heritage & van Niekerk, 1995) are characterized by dry tributaries and a concentration of river flow in single perennial channels

inclusion in a quartz grain at site 15, (d) columnar zircon inclusion in a quartz grain at site 14, (e) zoisite, olivine and clinopyroxene from site 3, (f) subhedral zoisite included in a quartz grain at site 9, with muscovite and biotite grains in the groundmass and present as inclusions within quartz grains, (g) tourmaline and quartz grains from site 10, (h) rutile inclusion in a quartz grain from site 5, (i) large rounded olivine grain and subrounded quartz grains from site 14, (j) orthopyroxene and clinopyroxene grains from site 3, (k) large orthopyroxene and clinopyroxene grains from site 1, (l) subhedral epidote grain from site 7, (m) subrounded olivine grain with plagioclase inclusions from site 15, (n) subhedral olivine grain which is slightly altered from site 9. Abbreviations are: bt = biotite, cpx = clinopyroxene, epd = epidote, msc = muscovite, olv = olivine, opx = orthopyroxene, plg = plagioclase, qtz = quartz, rt = rutile, tour = tourmaline, zirc = zircon, zoi = zoisite.

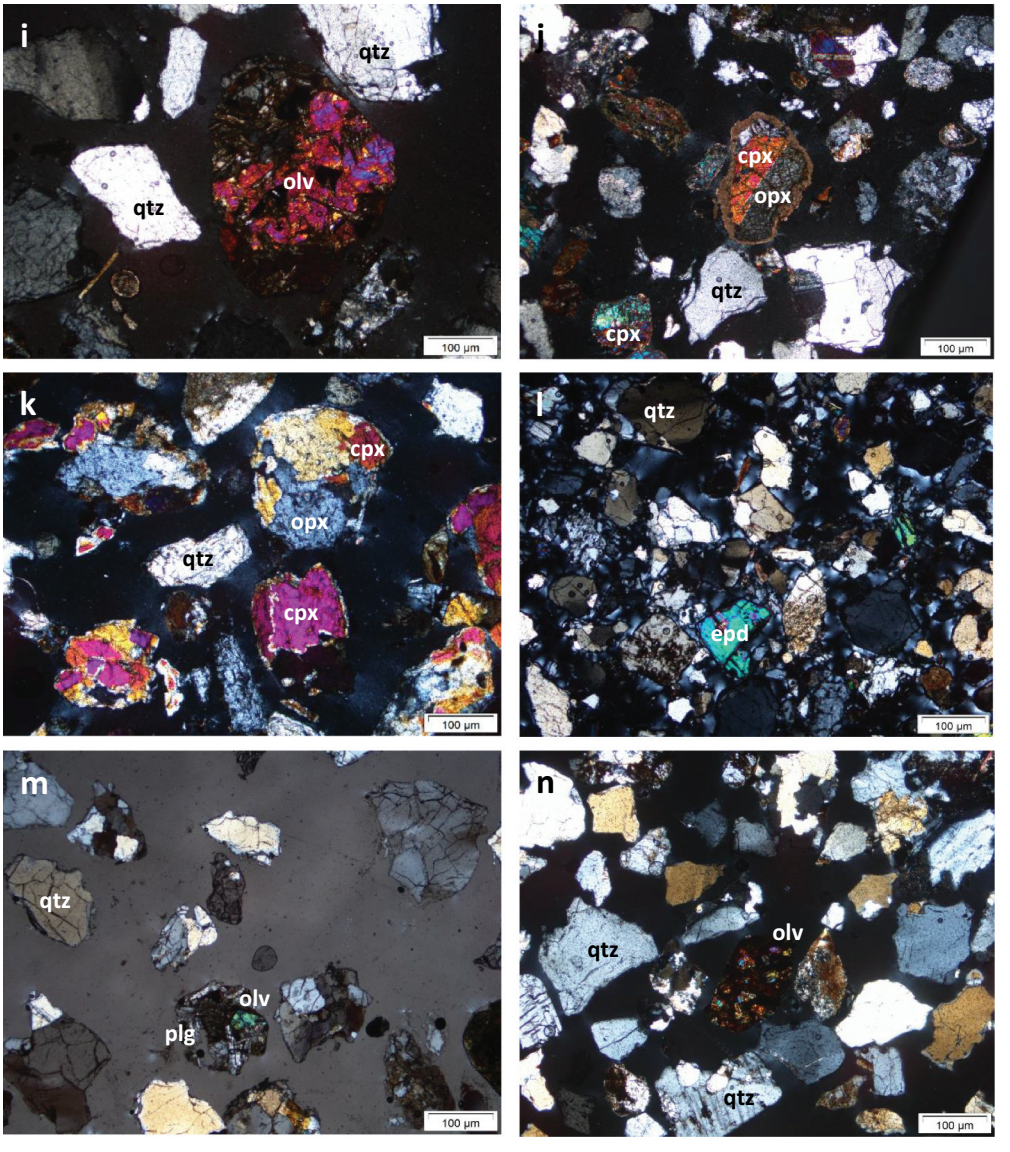


Figure 8. (Continued).

within the lowest part of the floodplain (Heritage & van Niekerk, 1995). Areas outside of the main channel are geomorphically inactive during low-flow conditions, except for small wind-formed dunes developed on the dry floodplains. Low-flow regimes are therefore characterized by very limited sediment movement except in association with channel bed sources (Knight & Evans, 2022). Flood regimes by contrast often activate the entire floodplain, as well as incoming tributaries, thereby drawing sediments from a wider range of source environments and from a wider geographical region. During floods, the very wide and relatively flat river channels and floodplain occupied by the Letaba River, such as at site 10 (Figure 5c), mean that sediments are derived by enhanced bank erosion, as well as from channel bed and tributary sources.

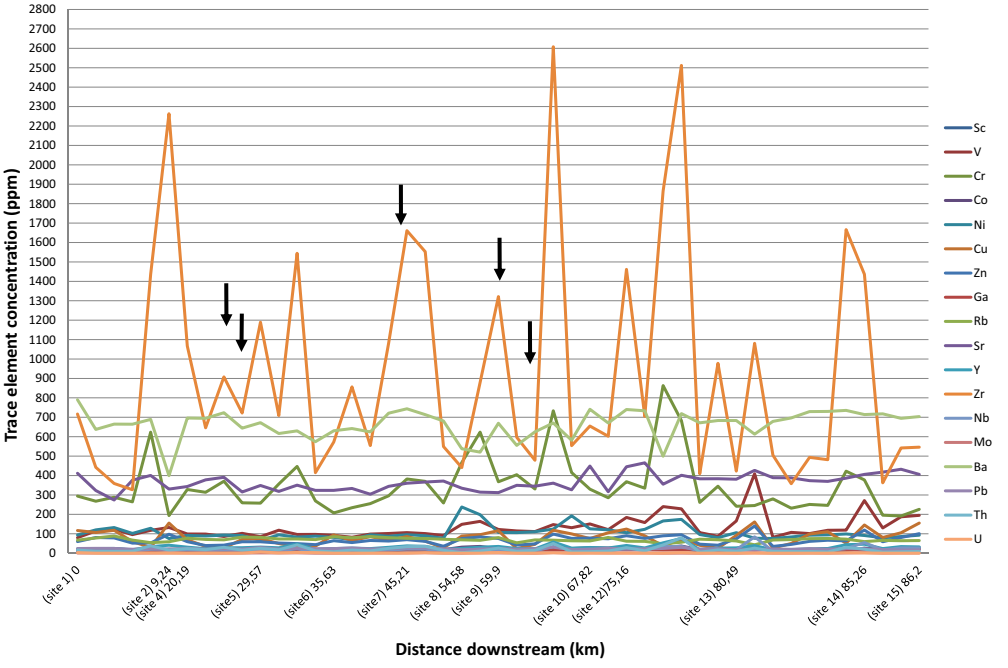


Figure 9. Graph indicating the trace elements and their abundance in different sediment samples in a downstream direction from site 1 from left to right. The arrows indicate the locations of major tributaries (Table 1). Precise values of trace elements are given in supplementary data file A.

Table 4. Summary of the contribution of different sediment sources (%) to surface river sediments found at sites 10–15. Note that no samples were analysed from site 11.

Site	Channel bank (%)	Channel bed (%)	Tributary (%)
10	27	51	22
12	13	77	10
13	62	21	17
14	12	77	11
15	28	48	24
Letaba River as a whole	22.5	42.5	35

The relative timing of river discharge response by non-perennial tributaries compared to the main channel depends on the spatial and temporal patterns of rainfall across the sub-catchments as well as any antecedent conditions. This means that tributaries can add new sediment into the main river channel with this sediment being incorporated into the main channel if this material is added during the main flood event (Figure 13). Alternatively, sediment accumulates adjacent to the tributary mouth within the main channel if this material is added at the end of the flood event or during waning flow conditions (e.g. Heritage & van Niekerk, 1995; Knight & Evans, 2022) (Figures 12 and 13). Thus, the sediment source-area contribution to river sediments depends not only on river system geometry (sediment availability *versus* bedrock control, floodplain width, valley margin/terrace height and degree of erosion), but also the interplay between main channel and tributary sources.

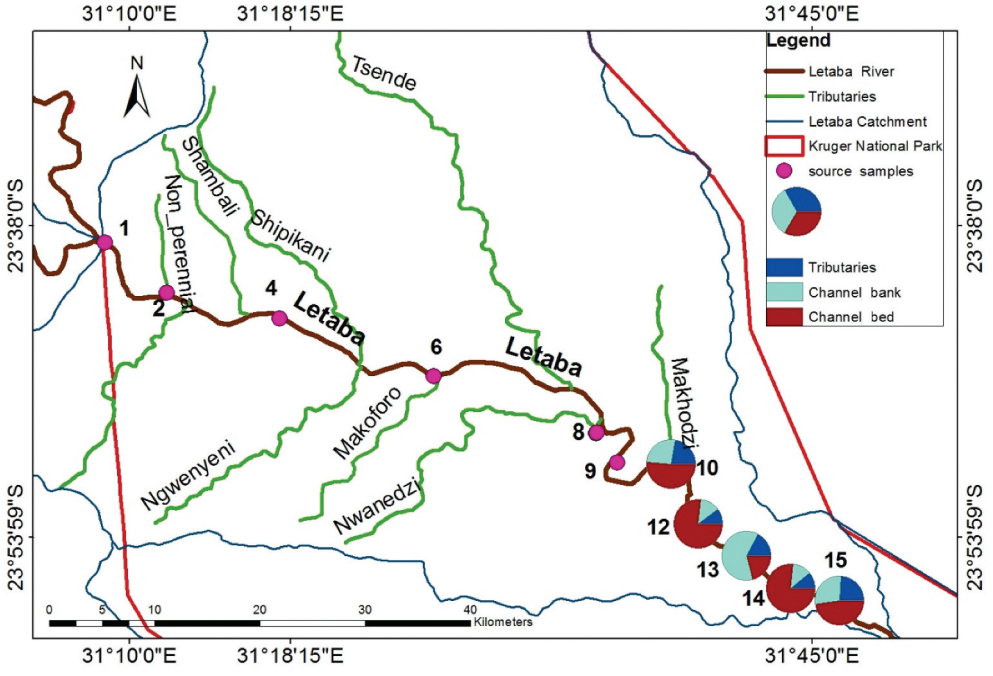


Figure 10. Map showing the contribution of tributary, channel bank and channel bed sources to downstream sites 10–15.

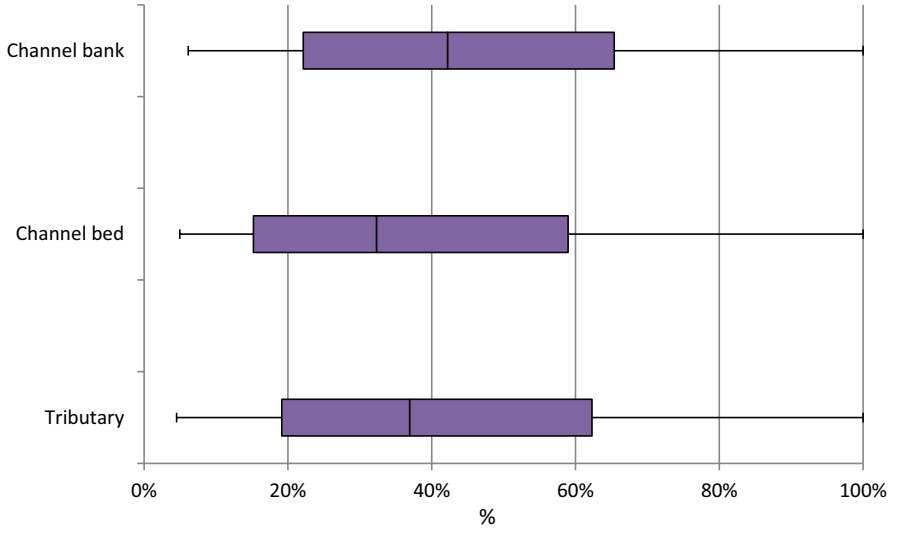


Figure 11. Whisker plot indicating the range of mean absolute errors obtained for samples derived from different source areas.

A model describing how sediment can be mobilized from different source areas under non-flood and flood situations in tributary and main channels is presented in Figure 12. This shows that under non-flood (or dry season) situations, sediments in active transit in the main river channel are reworked from the channel bed and sides. As river discharge increases, abandoned channels in the main river system become reactivated and sediments in transport are then derived from across the floodplain. When non-perennial tributaries are reactivated, a mix of sediments from across the (relatively narrow) valley, as well as the valley sides, are quickly added to the main river system (Figure 12c). In theory, this should mean that, at different periods of the flood wave, different sediment sources may become more dominant. In practice, however, previously deposited (and well-mixed) sediments are reactivated, and then mixed again with 'new' sediments, especially by floodwaters that tend to be highly energetic and turbulent. More organized patterns of sediment sorting tend not to occur until waning flow stages (Knight & Evans

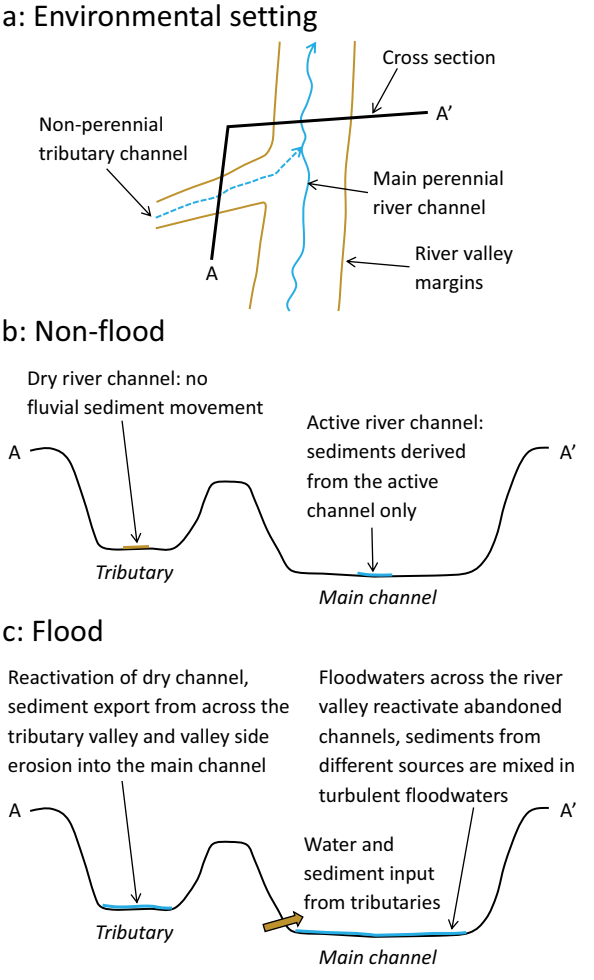


Figure 12. Model illustrating how sediments can be sourced from different parts of the river system in (b) non-flood and (c) flood situations.

, 2017). Based on an example of sediment source fingerprinting within a New Zealand river, Vale et al. (2020) showed that sediment source areas are quite different between the rising and falling limbs of the flood hydrography, depending on catchment topography and floodwater travel time.

Evidence for the interplay between tributary and main river channel sources can be seen in several locations. At the junction of the Groot Letaba and Klein Letaba (site 1), sediment deposition from the Klein Letaba branch has pushed the low-flow river channel to the far bank of the Groot Letaba (Figure 5(a)). This indicates a different timing and recession of the flood wave in different parts of the catchment, leading to smaller tributaries working out of phase with one another. Figure 13 provides some examples of the interplay between tributaries and main river channels. Evidence for later activity of the Klein Letaba compared to the Groot Letaba comes from the presence of sand bars at the river confluence, corresponding to progradational sheetflows from the Klein Letaba, and separated by a broad low-flow channel (which was dry at the time of sampling) (Figure 13(a)). This flood response can be compared with a similar situation on the Klaserie River, located north of the Letaba catchment in northeast South Africa. At the confluence of the Klaserie and the larger Olifants River, a subaqueous delta (100 m long, 220 m wide) shows that the Klaserie sediment system prograded into the Olifants during waning flow stages, pushing its own channel to the far bank and that the Klaserie tributary was active later than water flows in the main Olifants channel (Figure 13(b)). At the Klaserie mouth and preserved in an eroded bank is evidence for bidirectional ripple sets developed on a sand sheet reactivation surface and overlain by planar laminated sand (Figure 13(c)). This evidence reflects (i) individual flood waves within a single flood event, and (ii) the interplay between tributary-derived and main channel-derived flood waters, in which backing-up of water into the Klaserie tributary leads to upstream-migrating ripples overlain by a slackwater drape.

Variations in river discharge, therefore, have implications for the degree to which sediments may be reworked and the location from which reworked sediments are derived (Figure 12). River reaches with high sediment contributions from tributaries indicate the influence of high rainfall events on sediment delivery. The role of tributaries as the dominant source contributor diminishes in downstream reaches as sediments from channel sources are diluted over time (Figure 10). At downstream sites 12, 13 and 14, tributary sources contribute lower sediment percentages of 10%, 17% and 11%, respectively. Channel bed contributions are highest at sites 10, 12 and 14, with values of 51%, 77% and 77%, respectively (Table 4). The main control on sediment source contributions is reach-scale geomorphology, in particular the distribution of bedrock *versus* sediment across the floodplain (Knight & Evans, 2022; Milan et al., 2018). Although different river reach types are identified in the Letaba River (Figure 5), these cannot be uncritically matched to any particular patterns of sediment sources, since sediment found downstream has been reworked from upstream along sometimes unknown transport distances (cf., Pulley et al., 2020; Silva et al., 2016).

In terms of spatial patterns, site 10 has a 51% contribution from the channel bed, 27% from the channel bank and 22% from tributary sources (Table 4). The single straight channel of this river reach (Figure 5c) is favourable for channel bed erosion as the energy of the water is concentrated in a single place (Seidl & Dietrich, 1992). High water

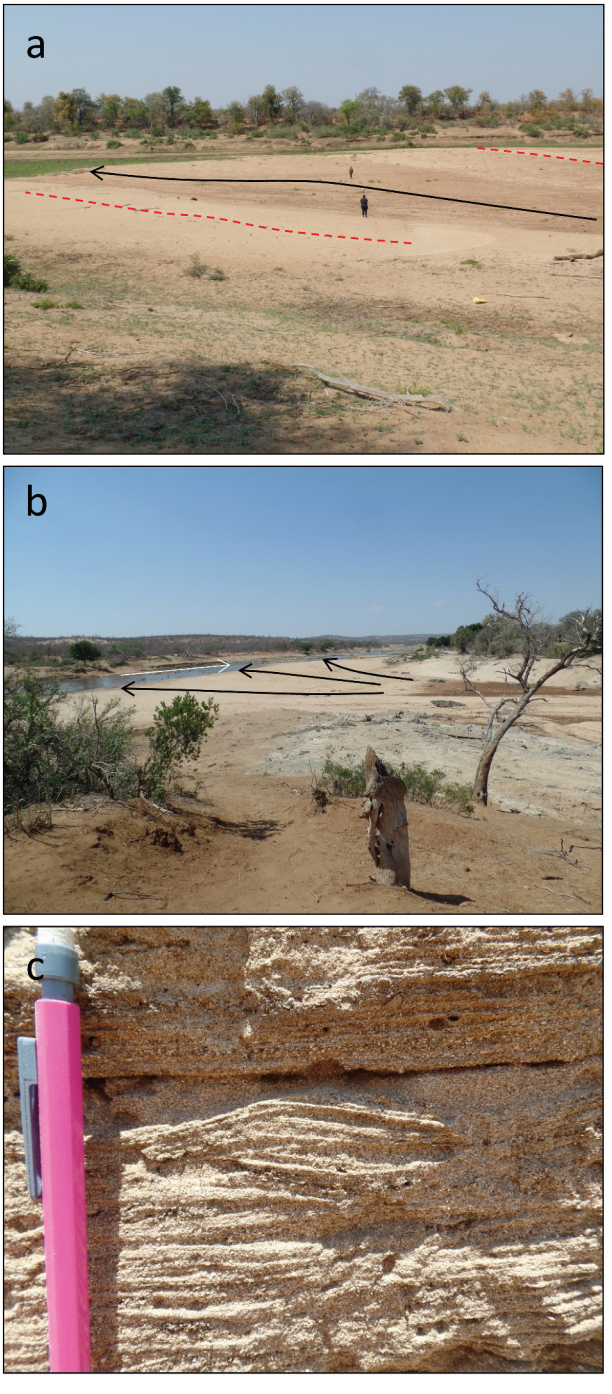


Figure 13. Examples of tributary–main channel interactions, discussed in the text. (a) Klein Letaba and Groot Letaba confluence, Letaba River (site 1 of this study). Sand bars (red dotted line) separate a low-flow thalweg (black arrow). (b) Junction between the Klaserie River (right) and the larger Olifants River (left, flow of the Olifants is towards the top right, location is at 24°04′51.3″S, 31°14′57.8″E). Waning floodwater from the Klaserie (black arrows) pushed out into the Olifants River (flow direction shown by white arrow). (c) Bidirectional ripples preserved at the Klaserie River mouth.

velocities can cause lateral erosion of the channel bank, resulting in a wider and deeper channel (Surian et al., 2016). The high contribution from channel bed sources (77%) at site 12 can be attributed to the influence of bedrock outcrops, which promote vertical incision by plucking during high flows (e.g. Allen et al., 2013; Seidl & Dietrich, 1992).

Only one site has a dominant contribution from the channel bank. At site 13, this contribution is 62%, and the lowest contribution of 17% from tributary sources (Table 4). This is a bedrock-influenced channel with very little sediment between the outcrops (Table 1). The river bank is also exposed at this reach, with no riparian vegetation present, facilitating erosion of the river bank. Site 14 has a high contribution (77%) from the channel bed. The channel bank contributes 12% and tributary sources 11% of the sediment. This river reach has a narrow channel and high sediment deposition on the floodplain upstream of the low-water bridge. This large mass of sediment suggests reworking and deposition from the channel bed. Channel bed sources also dominate at site 15, contributing 48% of the sediment (Figure 4(d)). There is also an increased contribution from the channel bank and tributary sources, at 28% and 24%, respectively. An increased contribution from tributaries can be explained by sediment storage on the floodplain of this river reach, eroded from upstream reaches.

5.2. Sediment sources and river dynamics

Landforms and heavy/trace elements recorded along the Letaba River are the signatures of sediment transport during flood events. Field mapping identified common geomorphic features within and alongside the low-water Letaba River channel, including flat-topped sand bars, 3D subaqueous dunes, overbank sand sheets and splays, inactive channels, gravel bars and lags, and in-channel sand bars (Figures 4 and 5). The presence of 3D subaqueous dunes is indicative of migrating bedload developed under high-energy conditions (Bartholdy et al., 2005; Knight & Evans, 2017) and sediment samples from these bedforms at site 1 show 25.8% and 58.8% very coarse and coarse sand, respectively, suggesting higher water velocities. Overbank sand sheets and splays are dominated by fine sediment, e.g. site 4 sample 2 is composed of fine (56.6%) and very fine (22.2%) sand, and site 9 sample 1 is composed of 94% fine sand.

Sediment properties (median grain size, sorting, skewness, kurtosis) do not change systematically downriver but median grain size decreases with distance from incoming tributaries (Figure 7 and Table 2), which likely reflects sorting during transport. There is also a slight trend towards negative skewness (coarser sediment) towards the end of the river (Figure 6). This may be an artefact of field sampling, but also that flood-transported sediment may be mixed by turbulence and then affected by hydraulic sorting during waning flow stages when sediment is deposited and landforms develop both within and outside of the active channel (Knight & Evans, 2017, 2018), leading to compartmentalization of different landforms and sediment sizes across the flood-affected valley (Figure 13). Some samples show indications of mixing of different sediment size populations: two samples from sites 5 and 15 are bimodally distributed which may reflect the mixing of saltating/bedload and suspended load during deposition. A change in underlying lithology may also influence skewness. For example, site 4 marks the local contact between diorite and granitic gneiss and marks a change from

positively to negatively skewed distributions due to the input of grains from the coarser granitic gneiss. This is also reflected in heavy mineral assemblages, which are related to the underlying geology and hydraulic processes during transport. Stable heavy minerals such as rutile, zircon, garnet and tourmaline are present in low quantities throughout, with concentrations ranging from less than 1% to 8.5% (Table 3). Derkachev and Nikolaevia (1995), Tsikouras et al. (2011) and Khalil et al. (2016) also identified these minerals in fluvial systems underlain by similar geologies as the Letaba River. Other common rock-forming minerals such as quartz, plagioclase and orthoclase are also present, with quartz being the most abundant, making up 36–55% of the samples. Differences in the sizes of minerals in different reaches are likely due to hydraulic sorting (Tsikouras et al., 2011), different transport distances, and sediment influx from different source areas (Garzanti et al., 2005). River bed microtopography (and thus bedform development) has been previously noted to affect the distribution of heavy minerals in South African rivers (Hattingh & Rust, 1992).

Trace element concentrations vary widely throughout the Letaba River (Figure 9). Background concentrations of trace elements in sediments are determined by the physical and chemical weathering of parent rock (Kabata-Pendias, 2011). Zirconium (Zr) is the most abundant element and is derived from weathering of zircon from igneous and metamorphic rocks (Thomas, 2011). This is supported by the strong positive relationship between zircon and Zr (0.61) (Supplementary data file B). The high specific gravity of zircon (4.0–4.7; Ďud'a and Rejl, 1986) may give rise to selective deposition along with low-density minerals such as quartz due to high flow velocities and turbulent flow (Rubey, 1933). High Zr concentrations of 2262 ppm and 1080 ppm were recorded at tributaries at sites 2 and 16, respectively. At site 6 (Makoforo River tributary), high concentrations of other trace elements decrease in a downstream direction.

A geomorphically informed analysis of sediment source areas reflects the processes and patterns of sediment erosion and transport taking place during floods, which are the most significant geomorphic agents along the Letaba and other semiarid rivers in northeast South Africa (Heritage et al., 2001b, 2001c, 2019; Milan et al., 2018; 2020). The three source areas identified and discussed in this study are reasonable given the geomorphic context, but it might be that a greater range of sources may inform on more complex spatial and temporal patterns of sediment transport by floods. It is unclear whether the results obtained from this study (Figure 13 and Table 4) are merely snapshots in time or whether the composition of different sediment sources reveals more fundamental insight into river sediment dynamics in particular in response to floods. For example, if certain reaches are dominated by sediments from certain erosional locations (banks, bed), then this may suggest that a genetic relationship exists between river reach geomorphology and their morphodynamic response during floods (Eze & Knight, 2018; Moon & Heritage, 2001). Several studies have shown genetic links between the geomorphology and morphodynamic behaviour of the adjacent Sabie River during flood events (e.g. Broadhurst & Heritage, 1998; Entwistle et al., 2014; Knight & Evans, 2022). This suggests that further sediment – landform analysis can inform on the detailed responses of semiarid rivers to variations in floodwater dynamics.

6. Conclusions

This study investigated sediment distributions and geomorphology within reaches along the Letaba River, South Africa, and the relative contributions to river sediment samples from different source areas within the catchment. Sediment patterns and sources are important because they influence the functioning of river systems. The increased sediment influx to the Letaba River associated with floods has given rise to an increased need to understand sediment patterns for the better management of river systems. The main findings of this research are:

- Relationships between sediments and landforms along different river reaches were examined to identify the main processes driving sediment distributions. Bedforms include sand bars on the floodplain, gravel bars, 3D subaqueous dunes and in-channel bars. The relationship of these landforms to high-energy flood events is supported by grain size, skewness, kurtosis and sorting values of the sediment samples which indicate the role of high-energy flow events in the transport and distribution of sediment within the river.
- The heavy minerals identified are characteristic of underlying rock types within the catchment. Hydraulic processes and selective deposition affect heavy mineral assemblages. Tributaries as potential sediment sources are seen in the high concentrations of trace elements of Cr, Ni, Zr, Ba and Cr. Correlation coefficients enabled relationships between trace elements from different source areas to be identified. Based on a simple mixing model, the overall greatest potential source of sediment within the Letaba River is from the channel bed (42%; Table 4), followed by tributaries (35%) and the channel bank (22%); however, this is highly variable between different sample sites along the main river. Sediments may be very rapidly reworked and mixed from these different areas during floods.
- Flood events are critical in reactivating non-perennial tributaries and adding new sediments into the main river channel. Measurements of in-channel sediment storage, therefore, do not give the whole picture of total sediment availability during floods (Heritage & Moon, 2000; Moon & Heritage, 2001) but highlight the critical role of flood events in the morphodynamic behaviour of semiarid rivers.

Future research directions may include a more detailed analysis of sediment geochemical properties and their downstream changes through the river system, with more closely spaced samples, or across the floodplain and in different landforms/elevations that may represent different flood events (e.g. Knight & Evans, 2018). Different tributaries/sub-catchments could also be geochemically characterized, as has been done elsewhere (e.g. Patault et al., 2019; Vale et al., 2022), to then be able to identify which sub-catchments are more dominant as sediment source areas under certain conditions.

Acknowledgements

The basis for this paper was fieldwork for the MSc dissertation of the third author, undertaken in 2015 and supervised by the first author. We thanks the anonymous reviewers for their comments on the submitted paper.

Disclosure statement

No potential conflict of interest was reported by the author(s).

Funding

This study was supported by NRF grant [91344] (to JK). We thank SANParks for permission to work in Kruger National Park (permit KNIGJ1225) and for logistic support.

References

Allen, G. H., Barnes, J. B., Pavelsky, T. M., & Kirby, E. (2013). Lithologic and tectonic controls on bedrock channel form at the northwest Himalayan front. *Journal of Geophysical Research: Earth Surface*, *118*(3), 1806–1825. https://doi.org/10.1002/jgrf.20113

Baade, J., Franz, S., & Reichel, A. (2012). Reservoir siltation and sediment yield in the Kruger National Park, South Africa: A first assessment. *Land Degradation & Development*, *23*(6), 586–600. https://doi.org/10.1002/ldr.2173

Bartholdy, J., Flemming, B. W., Bartholomä, A., & Ernstsen, V. B. (2005). Flow and grain size control of depth-independent simple subaqueous dunes. *Journal of Geophysical Research: Earth Surface*, *110*(F4), F04S16. https://doi.org/10.1029/2004JF000183

Blott, S. J., & Pye, K. (2001). Gradistat: A grain size distribution and statistics package for the analysis of unconsolidated sediments. *Earth Surface Processes and Landforms*, *26*(11), 1237–1248. https://doi.org/10.1002/esp.261

Bristow, J. W., Sweeney, R., & Venter, F. J. (1986). Geological guide to selected areas of the Kruger National Park. *Koedoe*, *29*(1), 183–202. https://doi.org/10.4102/koedoe.v29i1.530

Broadhurst, L. J., & Heritage, G. L. (1998). Modelling stage-discharge relationships in anastomosing bedrock-influenced sections of the Sabie River system. *Earth Surface Processes and Landforms*, *23*(5), 455–465. https://doi.org/10.1002/(SICI)1096-9837(199805)23:5<455:AID-ESP860>3.0.CO;2-2

Chadwick, O. A., Roering, J. J., Heimsath, A. M., Levick, S. R., Asner, G. P., & Khomo, L. (2013). Shaping post-orogenic landscapes by climate and chemical weathering. *Geology*, *41*(11), 1171–1174. https://doi.org/10.1130/G34721.1

Collins, A. L., & Walling, D. E. (2002). Selecting fingerprint properties for discriminating potential suspended sediment sources in river basins. *Journal of Hydrology*, *261*(1–4), 218–244. https://doi.org/10.1016/S0022-1694(02)00011-2

Collins, A. L., Walling, D. E., & Leeks, G. J. L. (1997). Use of the geochemical record preserved in floodplain deposits to reconstruct recent changes in river basin sediment sources. *Geomorphology*, *19*(1–2), 151–167. https://doi.org/10.1016/S0169-555X(96)00044-X

Collins, A. L., Walling, D. E., & Leeks, G. J. L. (1998). Use of composite fingerprints to determine the provenance of the contemporary suspended sediment load transported by rivers. *Earth Surface Processes and Landforms*, *23*(1), 31–52. https://doi.org/10.1002/(SICI)1096-9837(199801)23:1<31:AID-ESP816>3.0.CO;2-Z

Collins, A. L., Walling, D. E., Webb, L., & King, P. (2010). Apportioning catchment scale sediment sources using a modified composite fingerprinting technique incorporating property weightings and prior information. *Geoderma*, *155*(3–4), 249–261. https://doi.org/10.1016/j.geoderma.2009.12.008

Cooper, R. J., Krueger, T., Hiscock, K. M., & Rawlins, B. G. (2015). High-temporal resolution fluvial sediment source fingerprinting with uncertainty: A Bayesian approach. *Earth Surface Processes and Landforms*, *40*(1), 78–92. https://doi.org/10.1002/esp.3621

Cunningham, A. C., Evans, M., & Knight, J. (2015). Quantifying bleaching for zero-age fluvial sediment: A Bayesian approach. *Radiation Measurements*, *81*, 55–61. https://doi.org/10.1016/j.radmeas.2015.04.007

Dai, W., Chen, D., Li, M., Zeng, Y., Ni, L., Fang, N., & Shi, Z. (2022). Validating the accuracy of multiple sediment fingerprinting methods. *Land Degradation and Development*, *33*(18), 3965–3978. https://doi.org/10.1002/ldr.4437

Davies, J., Olley, J., Hawker, D., & McBroom, J. (2018). Application of the Bayesian approach to sediment fingerprinting and source attribution. *Hydrological Processes*, *32*(26), 3978–3995. https://doi.org/10.1002/hyp.13306

Derkachev, A. N., & Nikolaevia, N. A. (1995). Heavy mineral associations found in sediments of the East China Sea and adjacent Ryukyu and Taiwan areas. *Terrestrial, Atmospheric and Oceanic Sciences*, *6*(1), 75–90. https://doi.org/10.3319/TAO.1995.6.1.75(KEEP-MASS)

D'Haen, K., Verstraeten, G., & Degryse, P. (2012). Fingerprinting historical fluvial sediment fluxes. *Progress in Physical Geography*, *36*(2), 154–186. https://doi.org/10.1177/0309133311432581

Ďud'a, R., & Rejl, L. (1986). *Minerals of the World*. England: Spring Books.

Entwistle, N., Heritage, G., Tooth, S., & Milan, D. (2014). Anastomosing reach controls on hydraulics and sediment distribution on the Sabie River, South Africa. *IAHS Publication*, *367*, 215–219. https://doi.org/10.5194/piahs-367-215-2015

Erlank, A. J. (1984). Petrogenesis of the volcanic rocks of the Karoo Province. *Geological Society of South Africa*. Special Publication 13.

Eze, P. N., & Knight, J. (2018). A geomorphological characterisation of river systems in South Africa: A case study of the Sabie River. *Physics and Chemistry of the Earth*, *105*, 196–205. https://doi.org/10.1016/j.pce.2018.01.001

Folk, R. L., & Ward, W. C. (1957). Brazos River bar: A study in the significance of grain size parameters. *Journal of Sedimentary Petrology*, *27*(1), 3–26. https://doi.org/10.1306/74D70646-2B21-11D7-8648000102C1865D

Garzanti, E., Vezzoli, G., Andò, S., Paparella, P., & Clift, P. D. (2005). Petrology of Indus River sands: A key to interpret erosion history of the Western Himalayan Syntaxis. *Earth and Planetary Science Letters*, *229*(3–4), 287–302. https://doi.org/10.1016/j.epsl.2004.11.008

Grenfell, S. E., & Ellery, W. N. (2009). Hydrology, sediment transport dynamics and geomorphology of a variable flow river: The Mfolozi River, South Africa. *Water SA*, *35*(3), 271–282. https://doi.org/10.4314/wsa.v35i3.76764

Grenfell, S. E., Grenfell, M. C., Rowntree, K. M., & Ellery, W. N. (2014). Fluvial connectivity and climate: A comparison of channel pattern and process in two climatically contrasting fluvial sedimentary systems in South Africa. *Geomorphology*, *205*, 142–154. https://doi.org/10.1016/j.geomorph.2012.05.010

Haddadchi, A., Olley, J., & Laceby, P. (2014). Accuracy of mixing models in predicting sediment source contributions. *Science of the Total Environment*, *497–498*, 139–152. https://doi.org/10.1016/j.scitotenv.2014.07.105

Haddadchi, A., Ryder, D. S., Evrard, O., & Olley, J. (2013). Sediment fingerprinting in fluvial systems: Review of tracers, sediment sources and mixing models. *International Journal of Sediment Research*, *28*(4), 560–578. https://doi.org/10.1016/S1001-6279(14)60013-5

Hattingh, J., & Rust, I. C. (1992). Bed microtopography in a gravel-bed river and its influence on heavy mineral concentration. *South African Journal of Geology*, *95*(5–6), 159–164.

Heritage, G. L., Broadhurst, L. J., & Birkhead, A. L. (2001a). The influence of contemporary flow regime on the geomorphology of the Sabie River, South Africa. *Geomorphology*, *38*(3–4), 197–211. https://doi.org/10.1016/S0169-555X(00)00090-8

Heritage, G., Entwistle, N., Milan, D., & Tooth, S. (2019). Quantifying and contextualising cyclone-driven, extreme flood magnitudes in bedrock-influenced dryland rivers. *Advances in Water Resources*, *123*, 145–159. https://doi.org/10.1016/j.advwatres.2018.11.006

Heritage, G. L., Large, A. R. G., Moon, B. P., & Birkhead, A. L. (2003). Estimating extreme flood magnitude in bedrock-influenced channels using representative reach-based channel resistance data. *Geografiska Annaler*, *85A*(1), 1–11. https://doi.org/10.1111/1468-0459.00184

Heritage, G. L., Large, A. R. G., Moon, B. P., & Jewitt, G. (2004). Channel hydraulics and geomorphic effects of an extreme flood event on the Sabie River, South Africa. *Catena*, *58*(2), 151–181. https://doi.org/10.1016/j.catena.2004.03.004

Heritage, G. L., & Moon, B. P. (2000). The contemporary geomorphology of the Sabie River in the Kruger National Park. *Koedoe*, *43*(1), 39–55. https://doi.org/10.4102/koedoe.v43i1.207

Heritage, G. L., Moon, B. O., Jewitt, G. P., Large, A. R. G., & Rountree, M. (2001c). The February 2000 floods on the Sabie River, South Africa: An examination of their magnitude and frequency. *Koedoe*, *44*(1), 37–44. https://doi.org/10.4102/koedoe.v44i1.184

Heritage, G. L., Moon, B. P., & Large, A. R. G. (2001b). The February 2000 floods on the Letaba River, South Africa: An examination of magnitude and frequency. *Koedoe*, *44*(2), 1–6. https://doi.org/10.4102/koedoe.v44i2.171

Heritage, G. L., Tooth, S., Entwistle, N., & Milan, D. (2015). Long-term flood controls on semi-arid river form: Evidence from the Sabie and Olifants rivers, eastern South Africa. *IAHS Publication*, *367*, 141–146. https://doi.org/10.5194/piahs-367-141-2015

Heritage, G. L., & van Niekerk, A. W. (1995). Drought conditions and sediment transport in the Sabie River. *Koedoe*, *38*(2), 1–9. https://doi.org/10.4102/koedoe.v38i2.311

Hughes, A. O., Huirama, M. K., Owens, P. N., & Petticrew, E. L. (2022). Stream bank erosion as a source of sediment within New Zealand catchments. *New Zealand Journal of Marine and Freshwater Research*, *56*(4), 632–655. https://doi.org/10.1080/00288330.2021.1929352

Hughes, A. O., Olley, J. M., Croke, J. C., & McKergow, L. A. (2009). Sediment source changes over the last 250 years in a dry-tropical catchment, central Queensland, Australia. *Geomorphology*, *104*(3–4), 262–275. https://doi.org/10.1016/j.geomorph.2008.09.003

Jury, M. R. (2016). Climate influences on upper Limpopo River flow. *Water SA*, *42*(1), 63–71. https://doi.org/10.4314/wsa.v42i1.08

Jury, M. R., & Lucio, F. D. F. (2004). The Mozambique floods of February 2000 in context. *South African Geographical Journal*, *86*(2), 141–146. https://doi.org/10.1080/03736245.2004.9713818

Kabata-Pendias, A. (2011). *Trace elements in soils and plants,* (4th Ed ed.). Boca Raton: CRC Press.

Khalil, M. I., Khan, M. N. I., Kabir, M. Z., Majumder, R. K., Ali, M. I., Paul, D., & Islam, S. M. A. (2016). Heavy minerals in sands along Brahmaputra (Jamuna) River of Bangladesh. *International Journal of Geosciences*, *7*(1), 47–52. https://doi.org/10.4236/ijg.2016.71005

Knight, J. (2022). Geomorphology and landscapes of the Limpopo River system. In F. Eckardt (Ed.), *Landforms and lLandscapes of Botswana* (pp. 287–298). Cham: Springer.

Knight, J., & Evans, M. (2017). The sediment stratigraphy of a flood event: An example from the Sabie River, South Africa. *Catena*, *151*, 87–97. https://doi.org/10.1016/j.catena.2016.12.015

Knight, J., & Evans, M. (2018). Luminescence dating, sediment analyses, and flood dynamics on the Sabie River, South Africa. *Geomorphology*, *319*, 1–14. https://doi.org/10.1016/j.geomorph.2018.07.011

Knight, J., & Evans, M. (2022). Characterising the geomorphic dynamics of river systems: An example of the Sabie River, South Africa. *Koedoe*, *64*(1), a1700. https://doi.org/10.4102/koedoe.v64i1.1700

Knight, J., & Evans, M. (2024). Flood dynamics on the upper Letaba River, South Africa, deduced from luminescence dating. *South African Geographical Journal*, 1–23. https://doi.org/10.1080/03736245.2024.2333764

Kotschy, K. A., Rogers, K. H., & Carter, A. J. (2000). Patterns of change in reed cover and distribution in a seasonal riverine wetland in South Africa. *Folia Geobotanica*, *35*(4), 363–373. https://doi.org/10.1007/BF02803549

Lynn, W., Thomas, J. E., & Moody, L. E.(2008). Petrographic microscope techniques for identifying soil minerals in grain mounts. In A. L. Ulery & L. R. Drees (Eds.), *Methods of Soil Analysis: Part 5 – Mineralogical Methods* (pp. 161–190). Soil Science Society of America.

Manjoro, M., Rowntree, K., Kakembo, V., Foster, I., & Collins, A. L. (2017). Use of sediment source fingerprinting to assess the role of subsurface erosion in the supply of fine sediment in a degraded catchment in the Eastern Cape, South Africa. *Journal of Environmental Management*, *194*(1), 27–41. https://doi.org/10.1016/j.jenvman.2016.07.019

Milan, D., Heritage, D., Tooth, S., & Entwistle, N. (2018). Morphodynamics of bedrock-influenced dryland rivers during extreme floods: Insights from the Kruger National Park, South Africa. *GSA Bulletin*, *130*(11–12), 1825–1841. https://doi.org/10.1130/B31839.1

Milan, D. J., Tooth, S., & Heritage, G. L. (2020). Topographic, hydraulic, and vegetative controls on bar and island development in mixed bedrock-alluvial, multichanneled, dryland rivers. *Water Resources Research*, *56*(5), e2019WR026101. https://doi.org/10.1029/2019WR026101

Miller, J. K., Rowntree, K. M., Foster, I. D. L., Reinwarth, B., & Baade, J. (2022). Application of environmental magnetism to estimate source contribution by lithology to Kruger National Park reservoirs. *Hydrological Processes*, *36*(10), e14709. https://doi.org/10.1002/hyp.14709

Moon, B. P., & Heritage, G. L. (2001). The contemporary geomorphology of the Letaba River in the Kruger National Park. *Koedoe*, *44*(1), 45–55. https://doi.org/10.4102/koedoe.v44i1.185

Mugwabana, T. (2018). *Sediment patterns and source areas within the Letaba River, Kruger National Park, South Africa* [MSc dissertation]. University of the Witwatersrand

Munyati, C., Ratchibvumo, T., & Ogola, J. (2013). Landsat TM image segmentation for delineating geological zone correlated vegetation stratification in the Kruger National Park, South Africa. *Physics and Chemistry of the Earth*, *55–57*, 1–10. https://doi.org/10.1016/j.pce.2009.11.014

Nosrati, K., Collins, A. L., & Madankan, M. (2018). Fingerprinting sub-basin spatial sediment sources using different multivariate statistical techniques and the modified MixSIR model. *Catena*, *164*, 32–43. https://doi.org/10.1016/j.catena.2018.01.003

Odiyo, J., Makungo, R., & Nkuna, T. R. (2015). Long-term changes and variability in rainfall and streamflow in Luvuvhu River Catchment, South Africa. *South African Journal of Science*, *111*(7–8), 2014–2169. https://doi.org/10.17159/sajs.2015/20140169

Patault, E., Alary, C., Franke, C., & Abriak, N.-E. (2019). Quantification of tributaries contributions using a confluence-based sediment fingerprinting approach in the Canche river watershed (France). *Science of the Total Environment*, *668*, 457–469. https://doi.org/10.1016/j.scitotenv.2019.02.458

Pettit, N. E., Naiman, R. J., Rogers, K. H., & Little, J. E. (2005). Post-flooding distribution and characteristics of large woody debris piles along the semi-arid Sabie River, South Africa. *River Research and Applications*, *21*(1), 27–38. https://doi.org/10.1002/rra.812

Pollard, S., du Toit, D., & Biggs, H. (2011). River management under transformation: The emergence of strategic adaptive management of river systems in the Kruger National Park. *Koedoe*, *53*(2), 1011. https://doi.org/10.4102/koedoe.v53i2.1011

Pulley, S., Collins, A. L., & Laceby, J. P. (2020). The representation of sediment source group tracer distributions in Monte Carlo uncertainty routines for fingerprinting: An analysis of accuracy and precision using data for four contrasting catchments. *Hydrological Processes*, *34*(11), 2381–2400. https://doi.org/10.1002/hyp.13736

Pulley, S., van der Waal, B., Collins, A. L., Foster, I. D. L., & Rowntree, K. (2017). Are source groups always appropriate when sediment fingerprinting? The direct comparison of source and sediment samples as a methodological step. *River Research and Applications*, *33*(10), 1553–1563. https://doi.org/10.1002/rra.3192

Rountree, M. W., Heritage, G. L., & Rogers, K. H. (2001). In-channel metamorphosis in a semiarid, mixed bedrock/alluvial river system: Implications for instream flow requirements. *IAHS Publication*, *266*, 113–123.

Rountree, M. W., Rogers, K. H., & Heritage, G. L. (2000). Landscape state change in the semi-arid Sabie River, Kruger National Park, in response to flood and drought. *South African Geographical Journal*, *82*(3), 173–181. https://doi.org/10.1080/03736245.2000.9713711

Rubey, W. W. (1933). The size-distribution of heavy minerals within a water-laid sandstone. *Journal of Sedimentary Petrology*, *3*(1), 3–29. https://doi.org/10.1306/D4268E37-2B26-11D7-8648000102C1865D

Saraiva Okello, A. M. L., Masih, I., Uhlenbrook, S., Jewitt, G. P. W., van der Zaag, P., & Riddell, E. (2015). Drivers of spatial and temporal variability of streamflow in the Incomati River basin. *Hydrology and Earth System Sciences*, *19*(2), 657–673. https://doi.org/10.5194/hess-19-657-2015

Scholtz, R., Kiker, G. A., Smit, I. P. J., & Venter, F. J. (2014). Identifying drivers that influence the spatial distribution of woody vegetation in Kruger National Park, South Africa. *Ecosphere*, *5*(6), 71. https://doi.org/10.1890/ES14-00034.1

Schutte, I. C. (1986). The general geology of the Kruger National Park. *Koedoe*, *29*(1), 13–37. https://doi.org/10.4102/koedoe.v29i1.517

Seidl, M. A., & Dietrich, W. E. (1992). The problem of channel erosion into bedrock. *Catena*, *Suppl. 23*, 101–124.
Silva, M. M. V. G., Cabral Pinto, M. M. S., & Carvalho, P. C. S. (2016). Major, trace and REE geochemistry of recent sediments from lower Catumbela River (Angola). *Journal of African Earth Sciences*, *115*, 203–217. https://doi.org/10.1016/j.jafrearsci.2015.12.014
Smith, H. G., Karam, D. S., & Lennard, A. T. (2018). Evaluating tracer selection for catchment sediment fingerprinting. *Journal of Soils and Sediments*, *18*(9), 3005–3019. https://doi.org/10.1007/s11368-018-1990-7
Smith, A. M., & Zawada, P. K. (1990). Palaeoflood hydrology: A tool for South Africa? – an example from the Crocodile River near Brits, Transvaal, South Africa. *Water SA*, *16*(3), 195–200.
Spaliviero, M., De Dapper, M., & Maló, S. (2014). Flood analysis of the Limpopo River basin through past evolution reconstruction and a geomorphological approach. *Natural Hazards & Earth System Science*, *14*(8), 2027–2039. https://doi.org/10.5194/nhess-14-2027-2014
State of the Rivers Report. (2001). *Letaba and Luvuvhu river systems. WRC report TT 165/01*. Pretoria: Water Research Commission.
Surian, N., Righini, M., Lucía, A., Nardi, L., Amponsah, W., Benvenuti, M., Borga, M., Cavalli, M., Comiti, F., Marchi, L., Rinaldi, M., & Viero, A. (2016). Channel response to extreme floods: Insights on controlling factors from six mountain rivers in northern Apennines, Italy. *Geomorphology*, *272*, 78–91. https://doi.org/10.1016/j.geomorph.2016.02.002
Thomas, W. A.(2011). Detrital-zircon geochronology and sediment provenance. *Lithosphere*, *3*(4), 304–308. https://doi.org/10.1130/RF.L001.1
Tooth, S., Brandt, D., Hancox, P. J., & McCarthy, T. S. (2004). Geological controls on alluvial river behaviour: A comparative study of three rivers on the South African Highveld. *Journal of African Earth Sciences*, *38*(1), 79–97. https://doi.org/10.1016/j.jafrearsci.2003.08.003
Tsikouras, B., Pe-Piper, G., Piper, D. J. W., & Schaffer, M. (2011). Varietal heavy mineral analysis of sediment provenance, Lower Cretaceous Scotian Basin, eastern Canada. *Sedimentary Geology*, *237*(3–4), 150–165. https://doi.org/10.1016/j.sedgeo.2011.02.011
Vale, S. S., Fuller, I. C., Procter, J. N., Basher, L. R., & Dymond, J. R. (2020). Storm event sediment fingerprinting for temporal and spatial sediment source tracing. *Hydrological Processes*, *34*(15), 3370–3386. https://doi.org/10.1002/hyp.13801
Vale, S., Swales, A., Smith, H. G., Olsen, G., & Woodward, B. (2022). Impacts of tracer type, tracer selection, and source dominance on source apportionment with sediment fingerprinting. *Science of the Total Environment*, *831*, 154832. https://doi.org/10.1016/j.scitotenv.2022.154832
van Niekerk, A. W., Heritage, G. L., & Moon, B. P. (1995). River classification for management: The geomorphology of the Sabie River in the eastern Transvaal. *South African Geographical Journal*, *77*(2), 68–76. https://doi.org/10.1080/03736245.1995.9713594
Venter, F. J. (1986). Soil patterns associated with the major geological units of the Kruger National Park. *Koedoe*, *26*(1), 125–138. https://doi.org/10.4102/koedoe.v29i1.525
Viljoen, M. (2015). The Kruger National Park: Geology and geomorphology of the wilderness. In S. Grab & J. Knight (Eds.), *Landscapes and Landforms of South Africa* (pp. 111–120). Cham: Springer.
Walling, D. E., & Collins, A. L. (2000). *Integrated assessment of catchment sediment budgets: A technical manual*. Exeter: Department for International Development/University of Exeter.
Walling, D. E., Collins, A. L., & Stroud, R. W. (2008). Tracing suspended sediment and particulate phosphorus sources in catchments. *Journal of Hydrology*, *350*(3–4), 274–289. https://doi.org/10.1016/j.jhydrol.2007.10.047
Zawada, P. K. (1997). Palaeoflood hydrology: Method and application in flood-prone Southern Africa. *South African Journal of Science*, *93*(3), 111–132.